00216-01

NASA/FAA
En Route Data Exchange (EDX)
Phase 2 Field Evaluation
Final Report
(Period Jan. 2001 – Dec. 2001)

Prepared for:

FAA Aeronautical Data Link (ADL) Product Team

Ed Jones
David R. Schleicher

Seagull Technology, Inc.

Under:

FAA Prime Contract No. DTFA01-98-C-00081
Unitech, Inc., Purchase Order # DC-CG 143 Project # 9833-014
Seagull Project No. C216

December 2001

Acknowledgment

This field evaluation project report was produced for the Federal Aviation Administration Aeronautical Data Link (ADL) Program under NASA guidance as part of the planned NASA/FAA En Route Data Exchange Phase 2 Field Evaluation. Mr. Rich Coppenbarger of NASA Ames Research Center and Mr. Jeff Bass and Ms. Vonia Ashton-Grigsby of the FAA provided programmatic guidance. United Airlines (UAL) and Honeywell Technology have also performed key roles in the evaluation, along with a number of FAA and NASA staff and consultants.

The test has involved United Airlines (UAL) Boeing 777 aircraft with FMS-Aircraft Communications Addressing and Reporting System (ACARS) systems and communicating with an EDX CTAS prototype operated from a remote EDX Lab at NASA Ames Research Center, Moffett Field, CA, manned by FAA and NASA staff and consultants. NASA staff and consultants have participated both by making necessary modifications to the CTAS prototype and by collecting and analyzing the received data. Mr. Jerry Kelley of UAL and Mr. Steve Quarry of Honeywell lent valuable guidance and technical expertise to this effort.

This final report was produced by Seagull Technology, Inc., of Los Gatos, California, under Subcontract to Unitech, Inc. Mr. Jim Huizenga of Unitech administered the Seagull Subcontract. The authors recognize significant inputs from Mr. Rich Coppenbarger and Mr. Gerd Kanning of NASA and Mr. Rey Salcido of Raytheon. Mr. Ed Jones and Mr. David Schleicher collected a majority of the technical information, led the analysis, and wrote the bulk of this report. Mr. Darren Dow and Mr. Bill Bjorkman of Seagull performed the bulk of the data processing. Drs. C. George Hunter and Richard Bortins provided technical consultation assistance.

Table Of Contents

Index of Figures

NASA/FAA En Route Data Exchange (EDX)
Phase 2 Field Evaluation
Final Report as of December 31, 2001

1 Introduction

The FAA Aeronautical Data Link (ADL) product team is investigating integration of the airborne Flight Management System (FMS), Air Traffic Management (ATM), and the Airline Operational Control (AOC) through addressable datalink technologies. This integration is expected to improve NAS performance and allow for increased accommodation of airspace user preferences. In parallel, the NASA Ames Research Center is developing air traffic control decision support tools to enhance the capacity, efficiency, and flexibility of the National Airspace System (NAS). Enroute decision support tools evolving from the Center-TRACON Automation System (CTAS) [Ref. 1] will assist controllers in the efficient management of air traffic. These decision support tools will impact aircraft at all phases of enroute flight, including climb, cruise, and descent, with the goal of reducing deviations from the airspace user's preferred trajectory. Previous studies [Refs. 2,3,4,5] have identified a number of benefits that Enroute Data Exchange (EDX) can provide, including enhanced controller awareness, accommodation of user preferences, and enhanced performance of such decision-support tools.

The purpose of the overall FAA/NASA EDX Project is to investigate the feasibility and operational benefit of sharing information between users and the ATM System. A Phase 1 EDX effort evaluated the improvement in CTAS trajectory prediction performance with pre-departure data obtained from AOC flight planning resources. EDX Phase 2 is extending Phase 1 by exercising real-time data downlink from the aircraft/FMS to the CTAS decision support system, focussing on the one-way exchange (flight deck-to-ATM) of aircraft state, performance, preference, and intent data. Future phases will utilize two-way datalink capabilities with future CTAS functionalities to facilitate advanced concepts such as four-dimensional (4D) user-ATM trajectory negotiation.

This document is a Final Report covering Seagull Technology Inc.'s participation in the Phase 2 Field Evaluation study in accordance with its Project Plan finalized in the February 2000 Project Plan update [Ref. 6]. The report covers activities, results and findings as of December 31, 2001.

The work entails several distinct but related analyses:

1) an analysis of the FMS downlinked information in comparison to information obtained from current surveillance, modeling, and flight planning sources (**Input Comparison Analysis**);
2) a **Lateral Route Intent Analysis** that compares FMS intent as inferred from the downlinked Active and Active+1 waypoints versus the Host flight plan (with amendments);
3) a **Trajectory Prediction Analysis** that compares trajectories synthesized from FMS downlinked information versus current trajectory predictions from the CTAS tools; and

4) a **Conflict Detection Analysis** that compares anticipated performance of conflict detection and resolution decision support tools with and without FMS downlink.

The report begins with a brief description of the EDX Phase 2 data collection system and process (Section 2). Section 3 then presents the data analysis results, supported by appendices. Section 4 presents conclusions and recommendations, based on the results.

2 EDX Phase 2 Data Analysis Process

The EDX Phase 2 field evaluation involved the downlinking aircraft state, performance, preference, and intent data from United Airline's Boeing 777 FMS-ACARS-equipped operational airline flights through Denver ARTCC (ZDV) airspace. The downlink is accomplished over the existing VHF ARINC ACARS Data Network System (ADNS). The details of the EDX architecture have been presented previously in Refs. 6, 7 and 8, and are not repeated here.

The overall data analysis process is illustrated in Figure 1. The aircraft downlinked data are received from the ACARS Ground Station via modem to the EDX laboratory at NASA Ames Research Center, where they are retained in data files. The EDX data is made available to the Input Comparison Analysis and Lateral Route Intent Analysis activities, along with the other nominal trajectory prediction input data (Host data and RUC 2 data) that are normally used by CTAS. These analysis activities are discussed extensively in Section 3. To support the Trajectory Prediction Analysis, the input data are fed to a Baseline version and a specially modified EDX version of CTAS. Details of the EDX CTAS modifications are presented in Ref. 7, but basically the modifications allow CTAS to utilize EDX data in lieu of its nominal sources. The Trajectory Prediction Analysis analyzes the comparative outputs of the respective versions of the CTAS Trajectory Synthesizer (TS) module [9] to determine improvements relative to the observed truth trajectories.

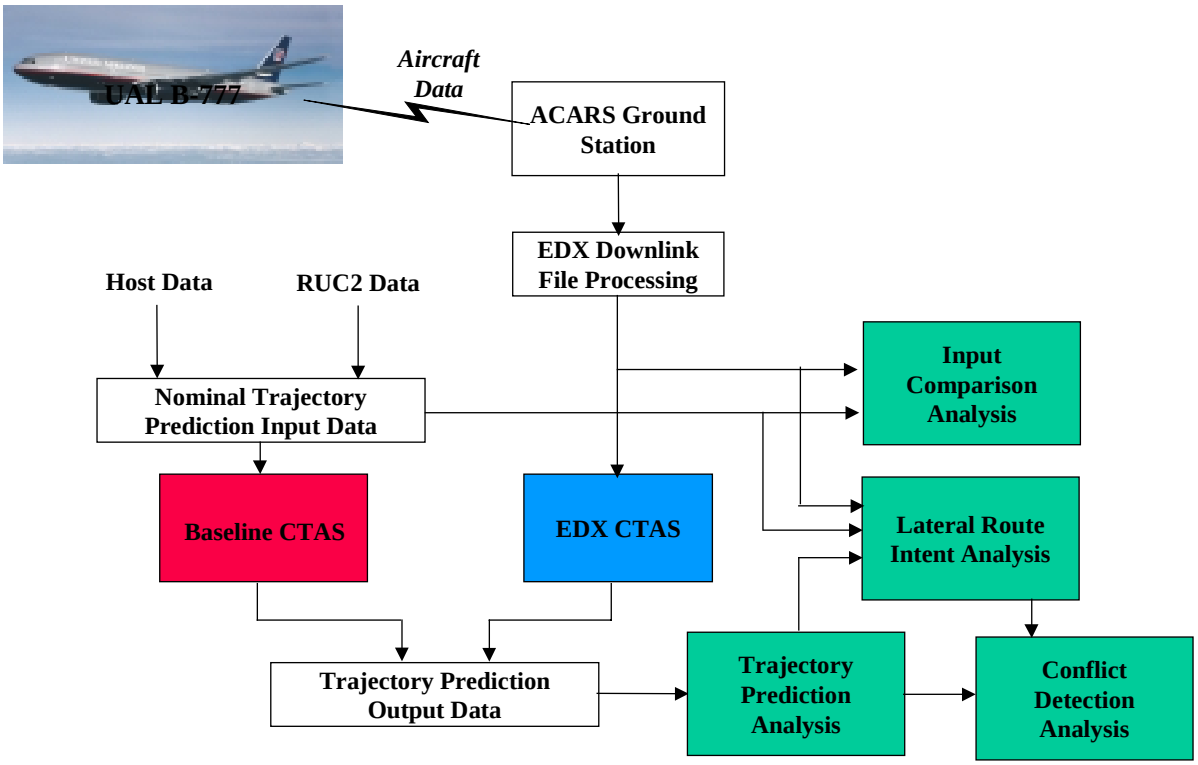

Figure 1 EDX Phase 2 Data Analysis Process

Forty-eight B777 aircraft were equipped with EDX downlink capability over the course of the EDX Project. The equipped EDX aircraft downlinked the primary parameters (shown in Figure 2) at a nominal rate of once per minute, along with a number of secondary parameters that may be useful in future analyses [10]. During occasional periods where few active EDX aircraft were present in the airspace, data link was increased up to a rate of once every 12 seconds in order to mirror the update rate of data from the FAA Center Host computer. The entire set of 40 parameters was packaged together into a single ACARS digital message totaling 192 bytes in length.

	Aircraft Parameter	Baseline CTAS Data Source
Aircraft State	UTC time stamp	CTAS clock
	Gross weight	Stored files
	Longitude - x	Radar data
	Latitude - y	Radar data
	Altitude - z	Mode-C transponder
	True track heading	Radar data
	Ground speed	Radar data
	Calibrated airspeed (CAS)	CTAS-computed
	True airspeed (TAS)	CTAS-computed
	Mach number	CTAS-computed
	Altitude rate	Radar data
	LNAV on/off	N/A
	VNAV on/off	N/A
Atmospheric State	Static air temperature	RUC2 model
	Static air pressure	RUC2 model
	Wind speed	RUC2 model
	Wind direction	RUC2 model
Flight Intent	Next (active) waypoint	ATC flight plan
	Next + 1 waypoint	ATC flight plan
	Target climb/descent CAS	Stored files
	Target climb/descent Mach	Stored files

Figure 2 Primary EDX Downlink Parameters [10]

3 Analysis Results

Several analyses were conducted on the data collected over the EDX field evaluation period. This report focuses on four distinct but related analyses:

1) an analysis of the FMS downlinked information in comparison to information obtained from current surveillance, modeling, and flight planning sources (**Input Comparison Analysis**);
2) a **Lateral Route Intent Analysis** that compares FMS intent as inferred from the downlinked Active and Active+1 waypoints versus the Host flight plan (with amendments);
3) a **Trajectory Prediction Analysis** that compares trajectories synthesized from FMS downlinked information versus current trajectory predictions from the CTAS tools; and
4) a **Conflict Detection Analysis** that compares anticipated performance of conflict detection decision support tools with and without FMS downlink.

3.1 Input Comparison Analysis

The Input Comparison Analysis examines the EDX data useful in trajectory prediction as compared to the traditional sources (Host, RUC 2, models) of such data. It is expected that the downlinked parameters will constitute a superior data source upon which to base prediction. Before presenting numerical results, a few observations are in order, provided that the data can be downlinked in a secure, reliable and timely manner.

Key Finding: Even with minimal engineering modifications and using the existing ACARS datalink (which was not specifically designed to meet the EDX vision), a wealth of aircraft data can be extracted with minimal avionics intrusion and transmitted reliably to ATC with minimal transit delay. Over an eight-month period, data were collected for over 1,000 operations within Denver ARTCC airspace, consisting of 288 Departures, 372 over-flights, and 341 Arrivals. Data link messages containing the EDX parameters were transmitted automatically for aircraft operating within 250 nmi of Denver International Airport. Because each EDX message was stamped with Coordinated Universal Time (UTC) aboard the aircraft, it was possible to measure the total delay associated with data transmission. For 60 randomly selected flights, involving an equal number of Departures, Overflights, and Arrivals, the average message delay was found to be 9 sec with a standard deviation of 12 sec [Ref. 10]. In processing the data using automatic "scripts," we found the data to be of high integrity, with instances of missing or unintelligible data being extremely rare.

Figure 2 has previously indicated the data sources used by the current Baseline CTAS as an example of the current technology in decision support tools. Referring to that figure, a number of the downlinked aircraft parameters are originally computed by the aircraft's navigation system, which is basically a GPS-aided Inertial Navigation System (INS). Such systems are highly accurate, being bounded (worst-case error) by the GPS. Accordingly, the downlinked positional and velocity state variables are expected to be more accurate than nominal GPS accuracy (15 meters RMS position, 0.1 knot RMS velocity), which will get considerably better as the Wide Area Augmentation System (WAAS) is more generally adopted. True track heading and groundspeed are also supplied by the GPS/INS navigation system. The onboard air data system

measures atmospheric parameters local to the aircraft, which should be clearly superior to the general models supplied by RUC 2, and the air data are used onboard to calculate high quality CAS, TAS and Mach information, which again should be superior to CTAS models.

The FMS also has first-hand knowledge of the whether lateral and vertical navigation modes (LNAV, VNAV) are engaged. This fact is highly related to FMS intent: the LNAV and VNAV modes are disengaged when the aircraft is being vectored, and the intended flight plan is not valid under these conditions. The baseline CTAS has no knowledge of navigation mode, so it can not adjust its trajectory predictions for periods when the flight plan is not valid due to vectoring, for example. Further, the FMS Active and Active+1 waypoints will be more current and valid as an indication of FMS lateral intent than the ATC flight plan, in general (this is the subject of the Lateral Route Intent Analysis, presented subsequently). In addition, the FMS target climb/descent CAS/Mach profiles will be a more accurate representation of the FMS vertical intent than the stored files generally used by CTAS.

Key Finding: EDX downlink of aircraft sensor and flight intent data can significantly reduce trajectory prediction errors for decision support tools. The Coppenbarger paper [Ref. 10] has presented the numerical results of the Input Comparison Analysis previously, but highlights of these results will be repeated here for completeness. Figure 3 shows a comparison of the EDX parameters with their corresponding baseline CTAS values as defined previously in Figure 2. Interestingly, the onboard weight estimate deviates from the baseline CTAS value by about 54,000 lbs. (on the mean) for Departures and Overflights, with quite a bit of variance (about 48,000 lbs. on Overflights). This level of deviation will have a marked effect on trajectory prediction, especially for Departures, as shown later in the Trajectory Prediction Analysis. The remainder of the aircraft state and atmospheric state parameters also show significant variations between the downlink and the corresponding values inferred from models or observed by Host radar. The flight intent errors indicated in the table are representative summaries that are elaborated upon extensively in the analyses to follow. The Mach and CAS parameters are addressed along with aircraft weight in the Trajectory Prediction Analysis of Section 3.3, and the Lateral Route Intent Error (LRIE) is addressed specifically in the Lateral Route Intent Analysis presented next.

The results in Figure 3 point to significant errors in the trajectory prediction data used today by ATC automation without the benefit of data link. Notably, the wind speed and aircraft velocity state errors are significant, and the standard deviation in the errors are also quite large, showing considerable dispersion in their distribution. Such errors should couple strongly into the ability to accurately predict trajectories, as examined more closely in the Trajectory Prediction Analysis to follow. In addition, the weight errors are sizable, particularly for Departures and Arrivals, and. Previous studies [11] have quantified such effects and noted major impacts in the ability to predict the climb-out altitude profile for weight errors of this magnitude.

Significant variations in FMS-downlinked weight were noted previously in [12] as well. Figure 4 presents an ensemble of the weight measurements and estimates of an ensemble of ten typical Departures as compared to the CTAS-assumed Departure weight. As shown, for these ten flights the FMS weight was consistently lighter than the CTAS assumption, by as much as about 20%. A discrepancy of this magnitude would certainly significantly impact TS climb-out trajectory predictions.

Parameter		Departures		Over-flights		Arrivals	
		Mean	*Std. Dev*	*Mean*	*Std. Dev*	*Mean*	*Std. Dev*
Aircraft State	Weight ($x10^3$lb)	53.9	20.3	53.8	47.7	18.9	13.4
	Gnd. speed (kt)	21	17.4	17	15.5	15	14.5
	CAS (kt)	19	13	25	26	20	16
	TAS (kt)	26	19	37	42	30	25
	Mach	.048	.03	.068	.069	.050	.041
	Alt. rate (ft/min)	345	495	85	124	390	487
	Track hdg. (deg)	3	3.23	2	3.73	6	15.7
Atmospheric State	Pressure (lb/ft^2)	7.6	12.1	1.1	0.6	10.1	10.5
	Wind speed (kt)	20	15	22	14	-	-
Flight Intent	Tgt. CAS (kt)	10	9	-	-	50	15
	Tgt. Mach	.047	.01	-	-	-	-
	LRIE (nmi)	1.12	1.16	.81	1.03	1.92	6.60

Figure 3 Input Comparison Analysis Results [10]

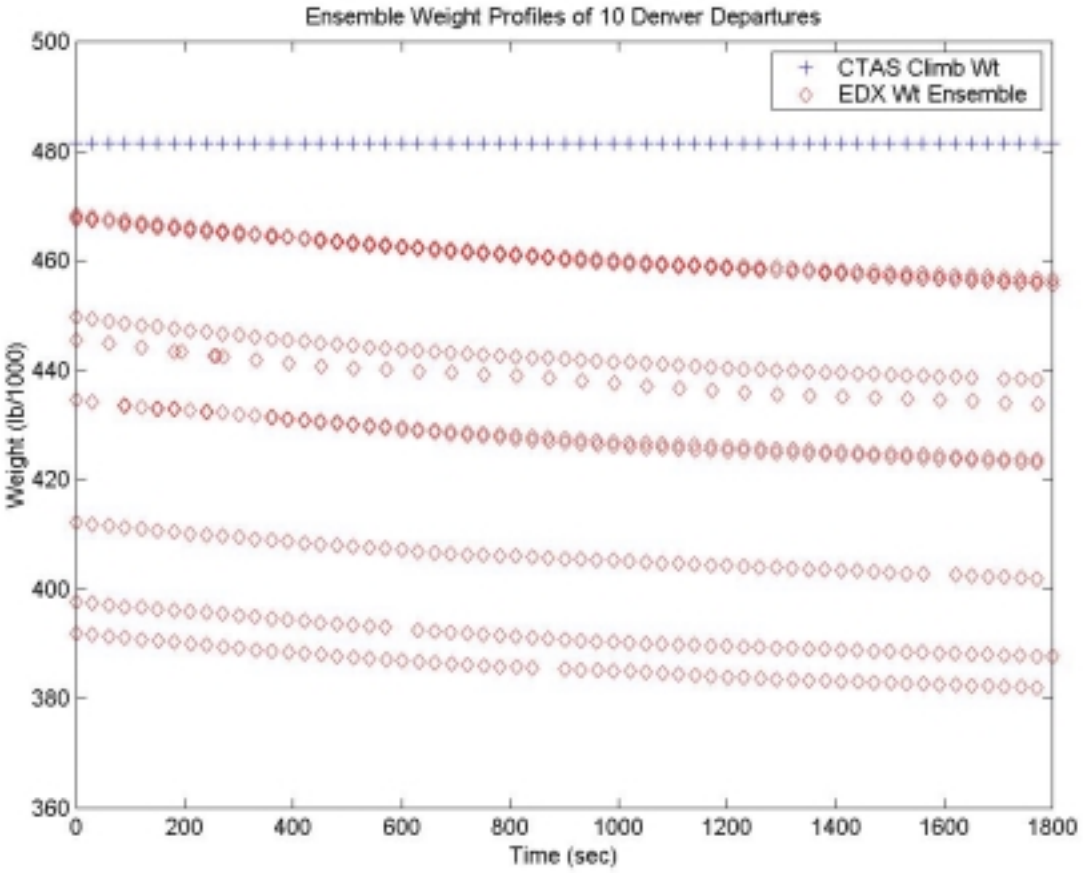

Figure 4 Weight Variations for 10 Representative Denver Departures [12]

3.2 Lateral Route Intent Analysis

The Lateral Route Intent Analysis compares the differences in the planned horizontal route constructed with and without the incorporation of EDX waypoint information from the aircraft FMS. Horizontal route intent was defined, at any given time, by connecting a path through all intended downstream waypoints. It should be noted that route intent is intrinsically dynamic in nature – Host route intent is affected by flight path amendments entered by the controller, while EDX route intent was affected by pilot inputs into the FMS.

Accordingly, the Host lateral intent at a given time was taken to be the original Host flight plan adjusted by any flight plan update messages received from the Host computer up to that point. The FMS lateral intent was inferred by adjusting the current instantaneous Host flight plan with the FMS Active and Active+1 waypoints as most recently received from the EDX data. Downstream of the FMS Active and Active+1 waypoints, it was assumed that the FMS flight plan rejoined with the instantaneous Host flight plan.

Key Finding: FMS lateral intent was often ambiguous in the data owing to the specific design choices of the downlink process, but ambiguities could be largely resolved through post processing. A major issue was discovered in this analysis having to do with the design of the downlink process. In the original planning, it was decided to use only four characters to represent waypoints. In reality, a large percentage of flights encountered 5-character waypoints, resulting in waypoint name ambiguities in the collected database. Fortunately, range and bearing to next waypoint were also downlinked, so we were able to resolve many of the ambiguities, especially in post-processing mode (real-time mode would only be able to resolve the next waypoint using range/bearing, and downstream predictions would still have problems). Naturally, we recommend that future implementations of FMS intent downlink use a 5-character representation for the waypoint name and continue to downlink next-waypoint range/bearing to further enhance data integrity. Further, we point out that it is important to synchronize the onboard and ground waypoint databases, again to ensure data integrity.

Trajectory Prediction Along Inferred Intent Path

To help automate the Lateral Route Intent Analysis, we developed a simple trajectory prediction model that would construct the Host lateral intent and FMS lateral intent at a given point in the trajectory, and predict the aircraft's path along that respective intended plan for a prescribed fly-out time into the future. We devised an analysis "script" that would begin at the first data point when both valid Host and valid FMS data were received, "fly-out" a prescribed prediction time into the future (nominally 20-minutes), and compute the Host lateral intent error and the FMS lateral intent error over that prediction window. The respective lateral intent errors were computed at each prediction point as the distance difference between the predicted intent point and the corresponding point on a path recorded from Host radar truth. Even though the downlinked GPS/INS position measurement is intrinsically more accurate, we used Host radar truth as a common basis to be consistent with the Baseline CTAS and EDX CTAS, which reset the prediction at each major cycle to the current radar position. The intent errors were resolved into cross-track and along-track components, relative to the radar truth path. We then advanced

the start point a prescribed time step (nominally 12 seconds to coincide with the normal Host update cycle), reset the current location to coincide with Host radar truth, and predicted the respective lateral paths and corresponding errors for the next prediction "window." This process was repeated until one of the data sources had been exhausted for that flight.

This prediction technique closely mimics the way that the CTAS trajectory synthesis model works, as illustrated in Figure 5, which compares the simple lateral prediction algorithm with the CTAS trajectory synthesizer operating on the same data set, in this case an Arrival to Denver from Indianapolis on March 11, 2001. Referring to the figure, the upper half shows the performance of the simplified trajectory prediction model as it projects along the Host flight plan and FMS intent as inferred from the downlinked Active and Active+1 waypoints. The Host flight plan is illustrated by the faint waypoints being followed by the Host (red) trajectory predictions. The FMS intent is being followed by the FMS (blue) trajectory predictions. In this case, as was typical, the FMS intent followed the truth trajectory (as measured by the Host radars) quite accurately (indistinguishable at the scale of the figure). The simplified prediction model attempts to accurately portray the waypoint switching logic employed by the CTAS Trajectory Synthesizer to correct itself when the Host flight plan is not being followed, as detected by the radars. This phenomenon is readily evident in the figure. The trajectory predictions are made repeatedly every time step, starting from the current location as measured by the radars. The switching logic applies rules to infer whether the current "next waypoint" truly represents intent, or whether the intended next waypoint should be switched to a downstream waypoint. As illustrated in the figure, the simplified logic does a credible job of emulating the CTAS waypoint-switching behavior. The one major difference is that the CTAS version appears to infer that the final waypoint switch is to a waypoint further downstream, probably the metering fix. Also notable is the curvature of the CTAS-predicted trajectories in comparison to the simplified model, which assumes straight-line flight between waypoints.

The successful emulation of the CTAS Trajectory Synthesizer is significant. It enabled us to examine a much greater number of flights than would have been practical using CTAS. The reason for this is that we could automatically execute the simplified model in a batch "script" that can operate on a large data set in "fast time," as opposed to the CTAS case where the trajectories need to be synthesized for each flight individually and executed in real time. Further, we were able to incorporate features into the analysis script that accommodates anomalies in the data, most notably, an accommodation of FMS waypoint ambiguities as discussed previously.

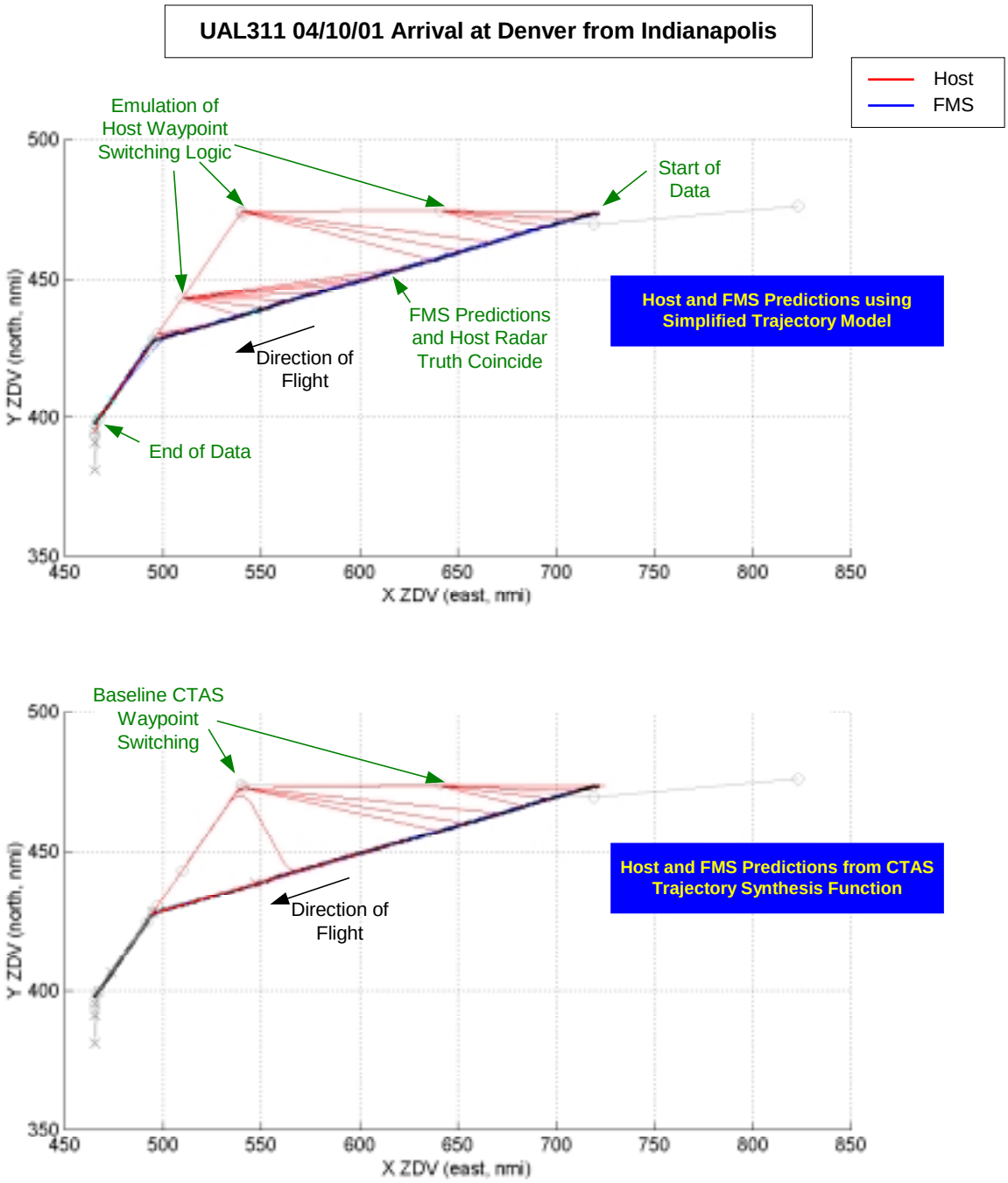

Figure 5 Typical Arrival Showing a Comparison of Trajectory Prediction Methods

Figures of Merit (FOMs)

The primary figures of merit (FOMs) for the Lateral Route Intent Analysis are the Host Lateral Route Intent Error (HLRIE) and FMS Lateral Route Intent Error (FLRIE). The HLRIE is defined as the difference between the radar truth trajectory and the Host flight plan (with updates) as extrapolated over a "projection window" (nominally 20 minutes to coincide with the planning horizons of typical decision support tools). Similarly, the FLRIE is defined as the difference between the radar truth trajectory and the inferred FMS intent as extrapolated over the projection window.

To calculate the differences between planned and actual trajectories over the projection window, we computed difference samples at a one-second interval and computed the mean and standard deviation of these samples over the projection window. Figure 6 illustrates the method of calculation of the HLRIE and FLRIE FOMs for a typical Arrival. Rather than potting all 20-minute projection windows, the figure only shows those windows where intent has changed. The beginning of such a window is indicated by a triangle on the respective truth trajectory. The cross-hatches between the respective curves represent the individual difference samples, which are averaged to calculate the FOMs. As illustrated, considerable vectored maneuvering under instruction by the Controller occurs near the end of the flight. This occurs commonly in Arrivals, and also occasionally in Departures and Overflights. The LNAV flag available in the FMS downlink is an indication of whether the FMS is engaged or the aircraft is being vectored. Accordingly, we ignored all windows when the LNAV flag indicated that the FMS was disengaged.

In addition to the magnitude of the HLRIE and FLRIE, the figures of merit were also resolved into cross-track and along-track components, relative to the radar truth path. The moving window average of all these FOMs was then calculated over each flight. In addition, we recorded which projection window exhibited the maximum HLRIE and FLRIE, and what that maximum value was. We also recorded which projection window contained the largest average HLRIE and FLRIE, and recorded that value as well.

We then grouped the flights into separate data sets for Arrivals, Departures, and Overflights and calculated ensemble means and ensemble standard deviations of all flights in the respective data set. In all, 191 Arrivals, 166 Departures, and 204 Overflights (561 flights in total) were analyzed in this way; the flights occurred from February through early April of 2001. Finally, we calculated "histograms" that show the distribution of how many flights in each category (Arrivals, Departures, Overflights) exhibited HLRIE and FLRIE FOMs in size "bins" ranging from less than 2 nautical miles (nmi) to over 50 nmi. Histogram analysis is explained more thoroughly in the next section.

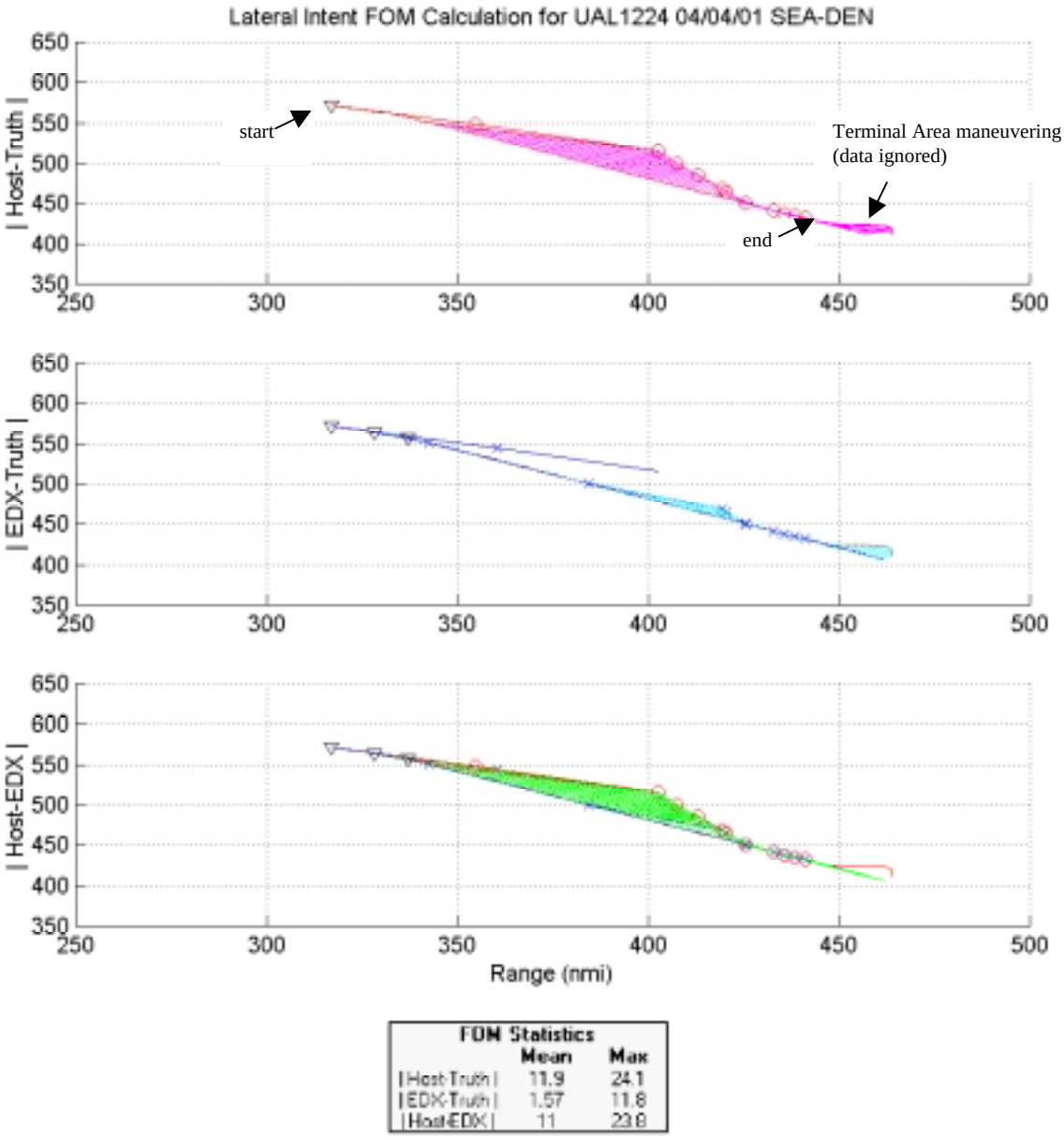

Figure 6 Illustration of Lateral Route Intent FOMs

Lateral Route Intent Analysis Key Results

A number of key results and findings from the Lateral Route Intent Analysis are now presented.

Key Finding: Downlinked FMS intent significantly reduces the average and maximum lateral intent error for Arrivals, Departures and Overflights. Figure 7 summarizes the average and maximum HLRIE and FLRIE for the 191 Arrivals, 166 Departures and 204 Overflights examined in the study. For Arrivals, the reduction in the average lateral route intent error is considerable – a reduction from over 6 nmi to 1.72 nmi. The ensemble standard deviation, which indicates the "dispersion" of the data about the mean, is also tightened up remarkably from 5.51 nmi down to 1.89 nmi. The averages are reduced considerable in the Departures and Overflights categories as well, although not quite as dramatically as the case with Arrivals. The improvements in the maximum columns are deceivingly conservative. Most of the maximum conditions for the downlinked FMS cases were very short-lived – they occurred primarily during times when FMS Active and Active+1 transitions were occurring. We believe that a more careful implementation of the FMS intent downlinking process would eliminate these transient effects.

	191 Arrivals				166 Departures				204 Overflights			
	Average		Maximum		Average		Maximum		Average		Maximum	
	HLRIE	FLRIE	HLRIE	FLRIE	HLRIE	FLRIE	HLRIE	FLRIE	HLRIE	FLRIE	HLRIE	FLRIE
Ensemble Mean (nmi)	6.06	1.72	16.24	11.09	2.46	1.53	7.79	6.06	1.09	0.47	4.35	2.78
Ensemble Std Dev (nmi)	5.51	1.89	11.44	9.96	2.32	1.89	8.65	6.24	1.48	0.59	6.01	5.04

Figure 7 Average and Maximum Lateral Route Intent Error for 561 Flights

Key Finding: A significant population of flights exhibit a mean Host Lateral Intent Error (HLRIE) greater than 4 nmi. While these ensemble statistics are interesting and representative of the overall improvement achievable by FMS intent downlink, it is even more revealing to look closely at the distribution of the number of flights with HLRIE levels in certain ranges. Figure 8 tabulates the population of Arrivals, Departures and Overflights that exhibited mean HLRIE values within the "bins" indicated (<2nmi, 2-4nmi, etc.). Figure 9 presents a histogram plot that portrays these results graphically. The histogram plot shows how many flights had a mean HLRIE within the various nmi ranges (nmi "bins"). As shown, over 54% of the Arrivals exhibited mean HLRIE values greater than 4 nmi. Correspondingly, 25% of the Departures and only 4% of the Overflights showed a mean HLRIE greater than 4 nmi. Notable in the histogram plot is the large population of Arrivals with HLRIE values in the 12 to 18 nmi bins. We believe this stems from a practice where the aircraft gets cleared to a downstream waypoint (probably the metering fix) – the FMS Active waypoint is updated in accordance with this clearance, but the Host flight plan is not updated for one reason or another.

Mean Host Lateral Route Intent Error (HLRIE)				
nmi	*Arrivals (Host)*	*Departures (Host)*	*Overflights (Host)*	*Total (Host)*
2	71	90	178	339
4	17	34	18	69
6	21	25	4	50
8	15	13	3	31
10	5	4	0	9
12	19	0	0	19
14	21	0	1	22
16	18	0	0	18
18	4	0	0	4
20	0	0	0	0
Total	191	166	204	561
%>4nmi	54%	25%	4%	27%

Figure 8 Population of Flights within Certain HLRIE Levels

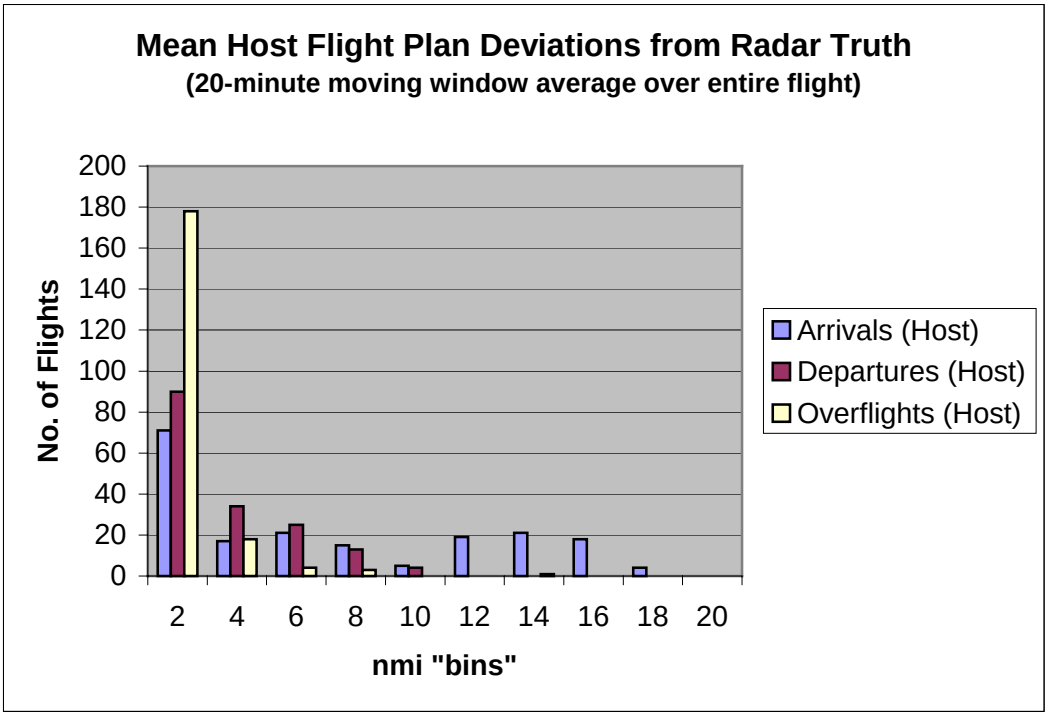

Figure 9 Histogram Plot of No. of Flights with Certain HLRIE Levels

Key Finding: Downlinked FMS Intent greatly reduces the population of flights exhibiting mean Lateral Intent Errors greater than 4 nmi. The analysis of FMS Lateral Intent Error (FLRIE) that corresponds to the HLRIE statistics presented above is summarized in Figure 10 and Figure 11. As shown, the number of Arrivals exhibiting mean FLRIE values greater than 4 nmi is reduced to 13% of the 191 population (compared to 54% for the HLRIE). For Departures, the mean FLRIE was reduced also to 13% of the 166 population (as compared to 25% HLRIE) and none of the Overflights showed a mean FLRIE over 4 nmi (as compared to 4% HLRIE). Also notable in the histogram plot (Figure 11) is that the population of Arrivals with HLRIE's in the 12-18 nmi bins is eliminated, as compared with Figure 9.

Mean FMS Lateral Route Intent Error (HLRIE)				
nmi	*Arrivals (FMS)*	*Departures (FMS)*	*Overflights (FMS)*	*Total (FMS)*
2	123	122	197	442
4	43	22	6	71
6	19	12	1	32
8	3	10	0	13
10	3	0	0	3
12	0	0	0	0
14	0	0	0	0
16	0	0	0	0
18	0	0	0	0
20	0	0	0	0
Total	191	166	204	561
%>4nmi	13%	13%	0%	9%

Figure 10 Population of Flights within Certain FLRIE Levels

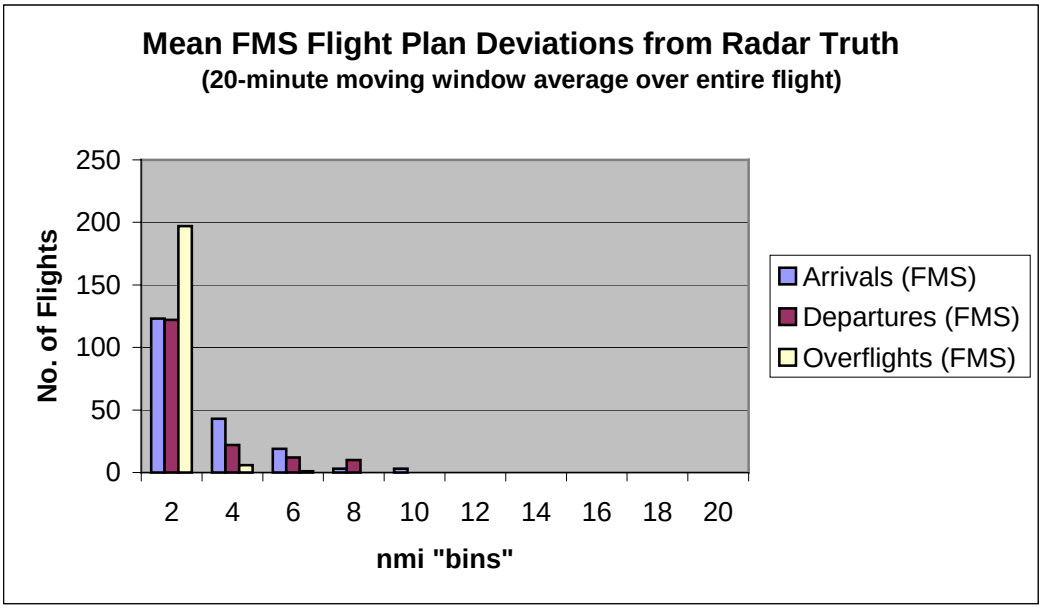

Figure 11 Histogram Plot of No. of Flights with Certain FLRIE Levels

The preceding analyses focused on a representative 20-minute projection window. An interesting point of investigation is to determine to what degree the FMS intent downlink (Active and Active+1 waypoints) supports a 20-minute planning window. Accordingly, for each 12-second time step through the data, we determined the amount of flight time represented by the Active and Active+1 waypoints from the present point at the present velocity. We then calculated the mean "look-ahead" time represented by the two FMS waypoints over the flight.

Key Finding: For Arrivals, the average look-ahead time represented by downlinked FMS Active and Active+1 waypoints was 13.2 minutes; for Departures and Overflights the corresponding average look-ahead times were 33.5 and 37.5 minutes, respectively. The distribution of average look-ahead times among Arrivals, Departures and Overflights is presented in Figure 12 and Figure 13. As shown, 51 of the 191 Arrivals (27%) exhibit an average look-ahead time of less than 10 minutes, and the largest population of Arrivals exhibit 15 to 20 minutes of FMS intent look-ahead. Only 30 Departures out of the 166 population (18%) exhibit average look-ahead times in the 15-20 minute range. The rest of the Departures and all the Overflights, on average, are covered by more than 30 minutes of flight by downlink of only two FMS waypoints.

minutes	*Arrivals*	*Departures*	*Overflights*	*Total Flights*
5 or less	0	0	0	0
10	51	0	0	51
15	84	12	0	96
20	52	18	18	88
30	4	64	57	125
40	0	28	49	77
50	0	15	37	52
60	0	12	34	46
More than 60	0	17	9	26

Figure 12 Population of Flights with Certain Average FMS Intent "Look-ahead" Times

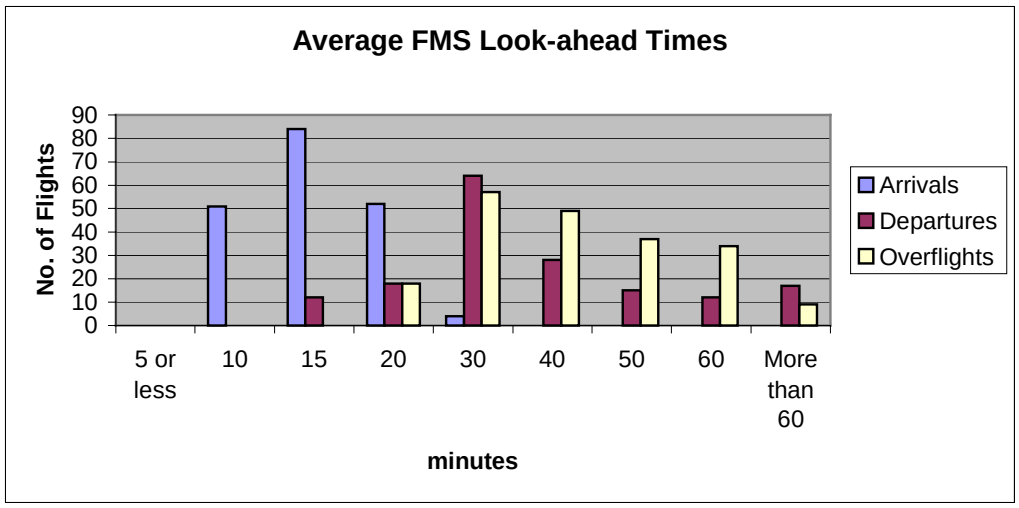

Figure 13 Histogram of Average Look-ahead Times Afforded by Two FMS Waypoints

3.3 Trajectory Prediction Analysis

The Trajectory Prediction Analysis compares trajectories synthesized from FMS downlinked information versus current trajectory predictions from the Baseline CTAS tools.

As described fully in Ref. 7, a number of significant changes were made to the Baseline CTAS in order to incorporate the downlinked FMS parameters. These changes included accommodation of FMS weight, CAS/Mach intent, and lateral route intent in the form of the FMS Active and Active+1 waypoints. The modified CTAS (termed the EDX CTAS) and the Baseline CTAS were then compared as regards the ability of the CTAS's internal Trajectory Synthesizer (TS) algorithm to predict the trajectory.

Since both the EDX CTAS and the Baseline CTAS were both designed only for real-time operation, it was time consuming to generate and analyze the data. Consequently, a selection was made of a sample set of 50 flights for this detailed Trajectory Prediction Analysis. For the selected flights, twenty-minute predictions, both with and without EDX data, were compared against truth - as established by the final track of the aircraft (radar truth).

Many of the Trajectory Prediction Analysis results were presented in Ref. 10, but selected results are presented here also, for completeness.

Twenty Departures were processed based on weight error; 10 Departures were processed based on speed intent error; and 20 Overflights were processed based on route intent error. In addition, the cumulative impact of weight and speed intent error was evaluated for the ten Departures examined for speed intent alone. For each flight, single 20-minute trajectory predictions were calculated with baseline-CTAS and EDX input parameters. In order to isolate the effect of the parameter in question, all other input parameters were set equal to baseline-CTAS values.

Key Finding: EDX downlink of FMS weight and flight intent parameters greatly improve the ability of decision support tools to predict the altitude profiles and lateral trajectory of the aircraft, as compared to radar truth. A comparison of the accuracy of EDX and baseline-CTAS trajectory predictions for the 50 flights is summarized in Figure 14. The results in Figure 14 show that EDX weight data alone improved the accuracy of predicted altitude by an average of nearly 30%. The incorporation of EDX speed intent improved the accuracy of predicted path distance by an average of 20%. Furthermore, the use of both EDX weight and speed intent improved altitude and path distance predictions by an average of 53% and 24%, respectively. For the 20-flight sample, the results in Figure 14 show an improvement in lateral path prediction accuracy of 60% with the use of EDX route intent data, provided in the form of FMS waypoints. This result is largely consistent with the average Lateral Route Intent Errors presented earlier in Figure 7 of Section 3.2, which used the simplified trajectory prediction algorithm to determine improvements of 72%, 38%, and 57% for 191 Arrivals, 166 Departures, and 204 Overflights, respectively.

Parameter(s)	Mean Altitude Error (ft)		Mean Lateral Error (nmi)	
	Baseline	EDX	Baseline	EDX
Weight	1,346	980	12	10.5
Speed Intent	1,360	1,160	12.3	10
Weight+Speed Intent	1,360	644	12.3	9.3
Lateral Route Intent	n/a	n/a	2.42	0.98

Figure 14 Impact of EDX Parameters on CTAS Trajectory Prediction Accuracy [Ref. 10]

As an illustrative example, Figure 15 shows the improvement in altitude profile prediction accuracy with the use of EDX data. Along with the baseline-CTAS prediction and actual track (truth), Figure 15 shows separate predictions based on the incorporation of 1) EDX weight, 2) EDX speed intent, and 3) EDX weight + speed intent. Figure 16 shows the corresponding path distance error measured for the same set of EDX and baseline predictions shown in Figure 15. It can be seen in Figure 16 that path-distance error was largely unaffected by aircraft weight. This observation is backed up by the equations of motion [9] which show that weight primarily influences the altitude dynamics, not path distance. Path distance error, however, was impacted by EDX speed intent, as expected.

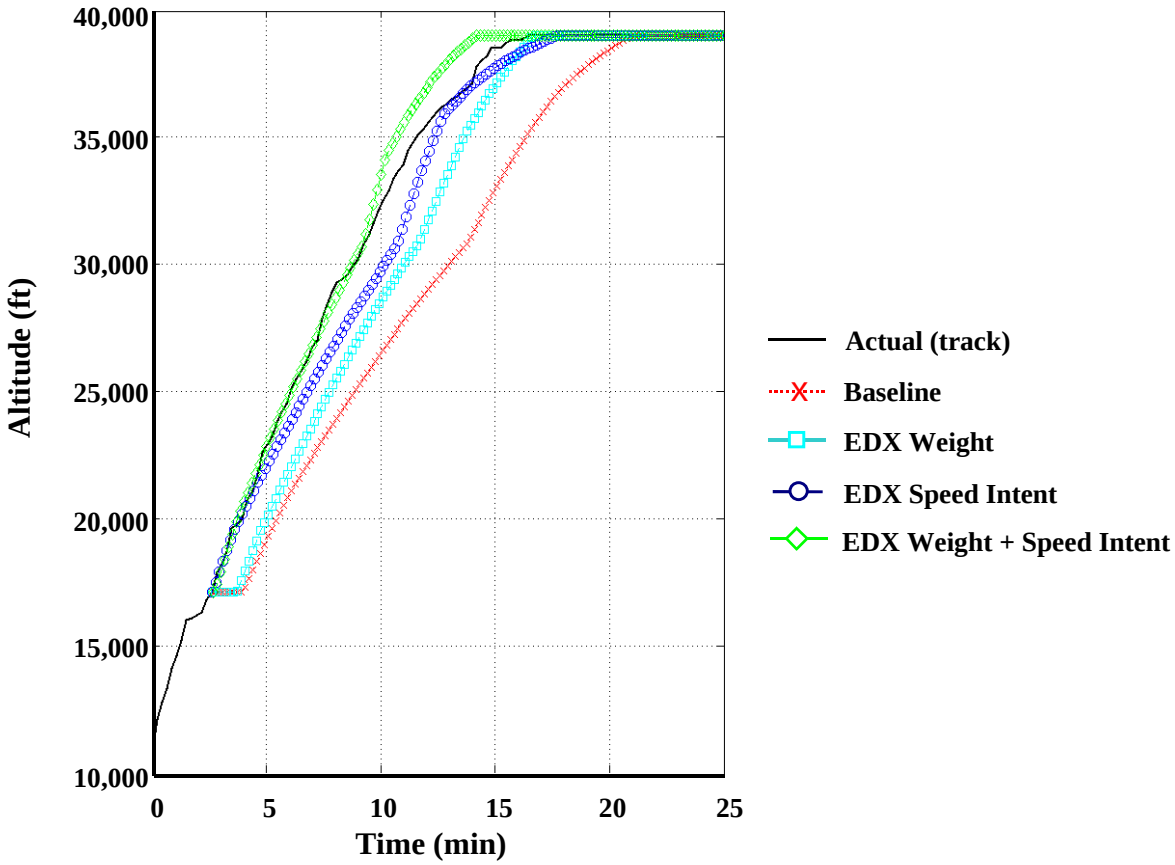

Figure 15 Effect of EDX Data on Predicted Altitude Profile Accuracy [10]

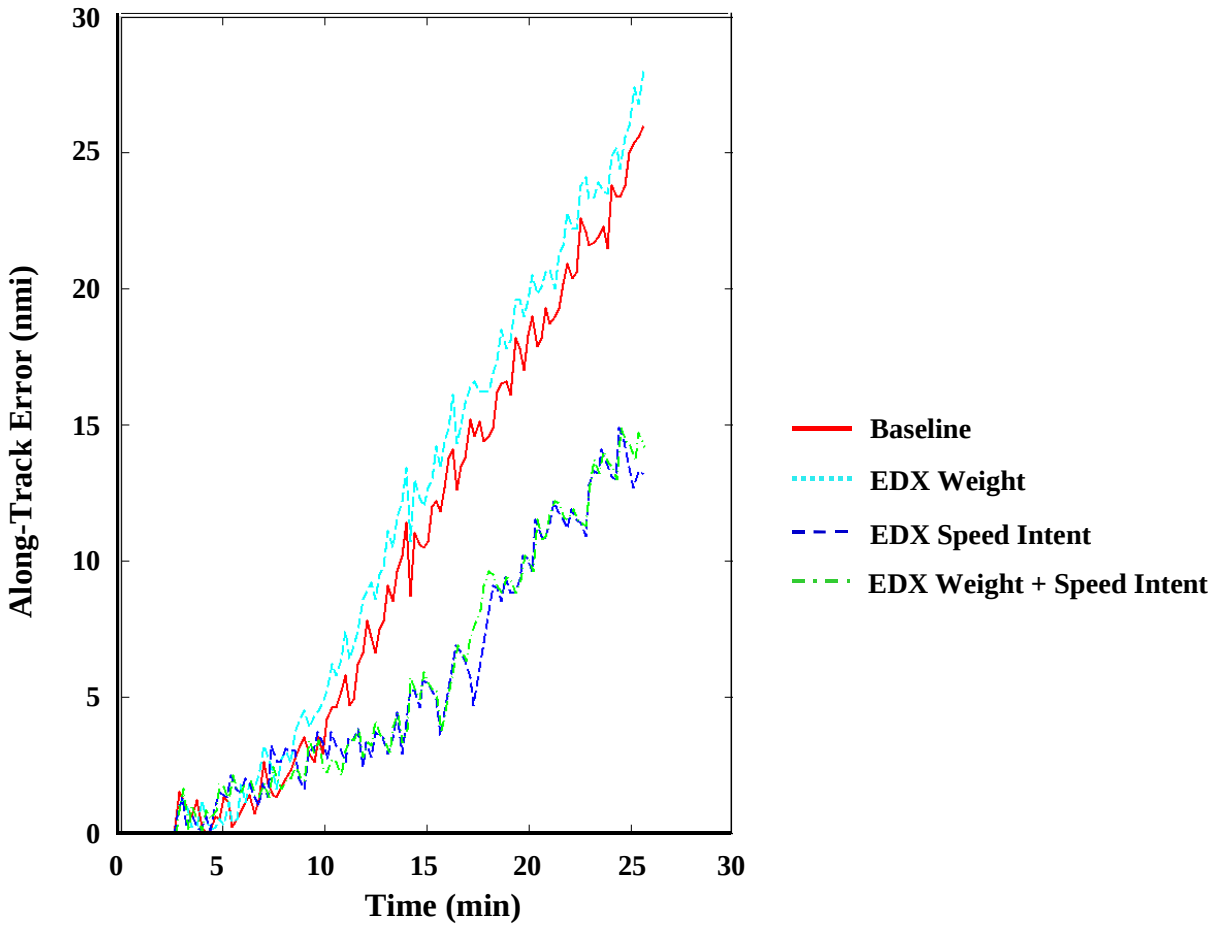

Figure 16 Effect of EDX Data on Predicted Path Distance Accuracy [10]

For this example flight depicted in Figure 15 and Figure 16, the maximum altitude error over a 20-minute prediction window was reduced by 73% with the incorporation of EDX weight and speed intent data. Similarly, the maximum path distance error was reduced by 60% with the incorporation of speed intent. It should be noted that the magnitudes of the error reductions in both altitude and in-trail path dimensions of the trajectory are well beyond the separation standards of low altitude en route airspace flight (1,000 ft and 5 nmi in altitude and path, respectively). This leads to the conclusion that EDX data could significantly influence ATC automation advisories and controller decisions relating to conflict avoidance and traffic flow management.

For the lateral case, Figure 17 shows an example of the improvement in lateral routing intent possible with the receipt of aircraft FMS waypoint information. In this example, the FMS data indicated that a direct route was to be flown from fix 1 to fix 3, thereby bypassing a dog-leg introduced by fix 2 in the filed flight plan. As shown in Figure 17, truth data, gathered post-flight, was used to validate FMS route intent. Figure 18 shows the total horizontal error corresponding to the predictions in Figure 17. Figure 18 indicates a reduction in maximum

horizontal prediction error of over 95% with the use of EDX aircraft data, for this particular 20-minute prediction example.

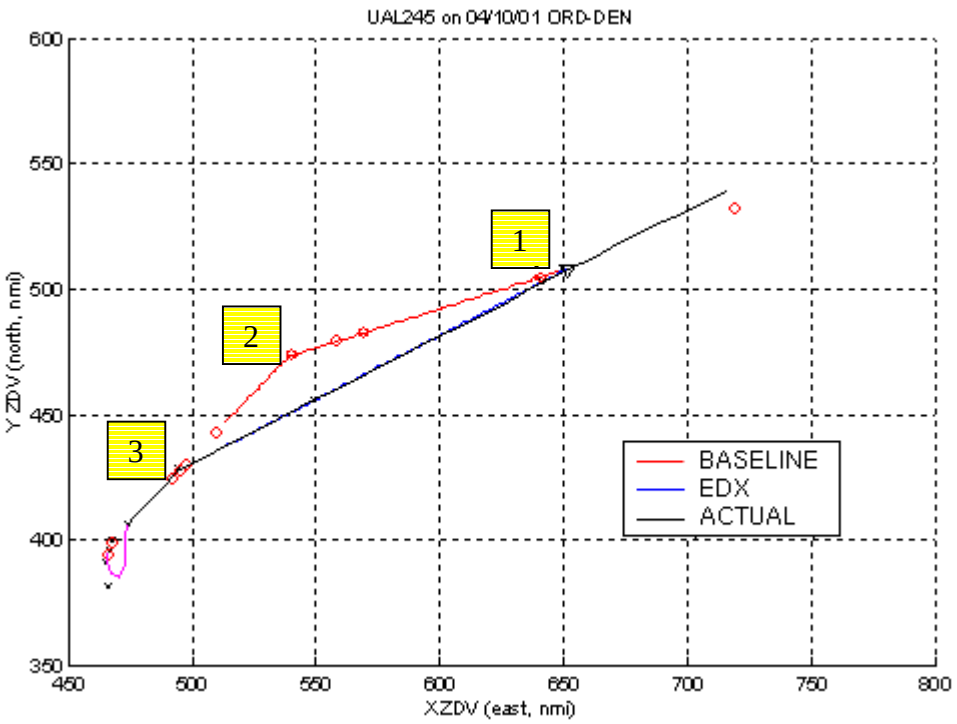

Figure 17 Impact of EDX Lateral Route Intent Data on Course Prediction Accuracy

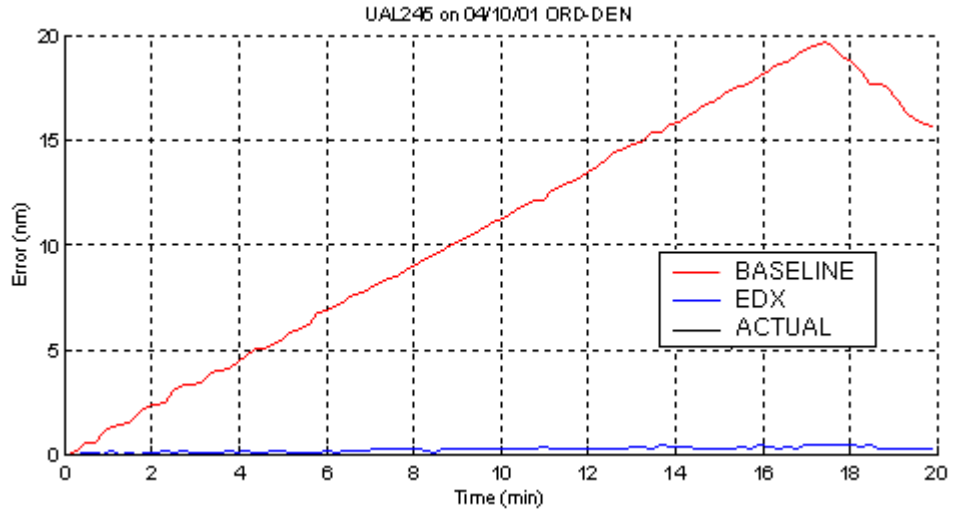

Figure 18 Impact of EDX Lateral Route Intent Data on Lateral Prediction Error

3.4 Conflict Detection Analysis

The use of EDX downlinked data by future ATM automation conflict probes will improve the accuracy of conflict detection methods. Current technology conflict probes have to contend with the inherent inaccuracies of radar-based position and velocity measurement and the limitations of Host flight plan data when controllers do not keep the Host computer intent model up to date. Downlinked data from an aircraft's FMS should offer considerable increases in current position, current velocity, and intent accuracy.

Existing Position, Velocity, and Intent Data Accuracies

In flight, FMS-equipped jet aircraft position and ground speed errors will typically be based on sophisticated inertial and GPS avionics onboard. On the ground, the accuracy of ATC sensing of aircraft position and speed will be limited to ground radar sensing and data processing systems. Typical GPS-derived and Radar-derived one-sigma surveillance errors are shown in Figure 19.

	GPS-derived	*Radar-derived*
Position error, σ_p (nmi)	0.0055[1]	0.45[2]
Ground Speed error, σ_v (nmi/min)	0.0042[3]	0.26[4]

[1]based on 10.2 m Selective Availability(SA)-off, GPS horizontal position error from [13]
[2]assuming measurement uncertainty based on mosaiced Air Route Surveillance Radar (ARSR) radar from 100 x 100 nmi range [14]
[3]based on 0.13 m/s Selective Availability(SA)-off, GPS ground speed error performance from BAE Systems ALLSTAR GPS receiver [15]
[4]based on 15.5 kt standard deviation Overflight ground speed error in **Figure 3**.

Figure 19 Typical FMS and Host-derived Current Position and Velocity Errors

Specific current position and velocity errors will be a function of a plethora of factors including (for GPS-derived data): the relative positions of a GPS receiver and the satellites it is tracking; and (for radar-derived data): range and azimuth from radars, single-sensor vs. mosaicing, radar registration, non-Mode C altitude estimation, antenna tilt and skew, refraction, coordinate conversion and timing uncertainties. In general, these errors will range significantly based on scenario-specific factors. For example, radar-derived position error will typically vary between 0.15 nmi to 0.9 nmi based purely on range from the radar source [14]. However, as one surmises from Figure 19, the typical radar-derived data current position and velocity errors are on the two orders of magnitude greater than that derived by using GPS data.

In addition to the improved state information, better predictions on lateral intent due to downlinked FMS-based intent data should improve conflict probe prediction accuracy. Previous investigations have shown the percentage of route clearances reflected in Host flight plan amendments to be as low as 18% [16]. Using the EDX and Host flight plan intent data collected during the Phase 2 field test, one may derive an intent-based predicted position error, σ_i, as a function of lookahead time. The method used for determining σ_i is as follows. For a given

aircraft flight and lookahead time, the Simple Trajectory Prediction Model (explained in Section 3.2) was used to project an aircraft forward in time, a given τ minutes ahead, along its flight plan. (Note: the varying ground speed in our predictions match the actual sensed ground speeds, and, therefore, uncouples the prediction error based purely on horizontal intent from that based on the ground speed.). Then, at time τ, the aircraft's actual position (based on Host radar data) was compared with the aircraft's predicted position and the relative position (with distance, D, and lateral and longitudinal components, x and y, respectively), were determined (see Figure 20). (Note: because of the ground speed matching, lateral deviations over time result in both cross-track and along-track position errors.)

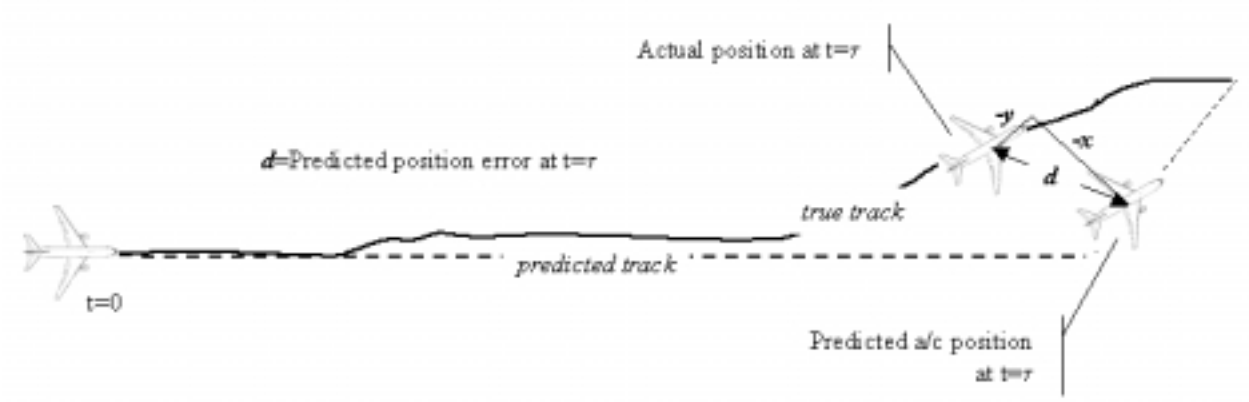

Figure 20 Intent-based Predicted Position Error Determination

This data was then collected for:

- all valid lookahead time windows from 5 to 30 minutes,
- Arrival, Departure, Overflights, and all aircraft flights,
- EDX and Host flight plan-based intent data, and
- only cases where the LNAV flag was "on" (Note: future conflict probes that receive LNAV "off" information are presumed to revert to a velocity-vector-based trajectory prediction),

and displayed on predicted position scatterplots. Example scatterplots are shown in Figure 21.

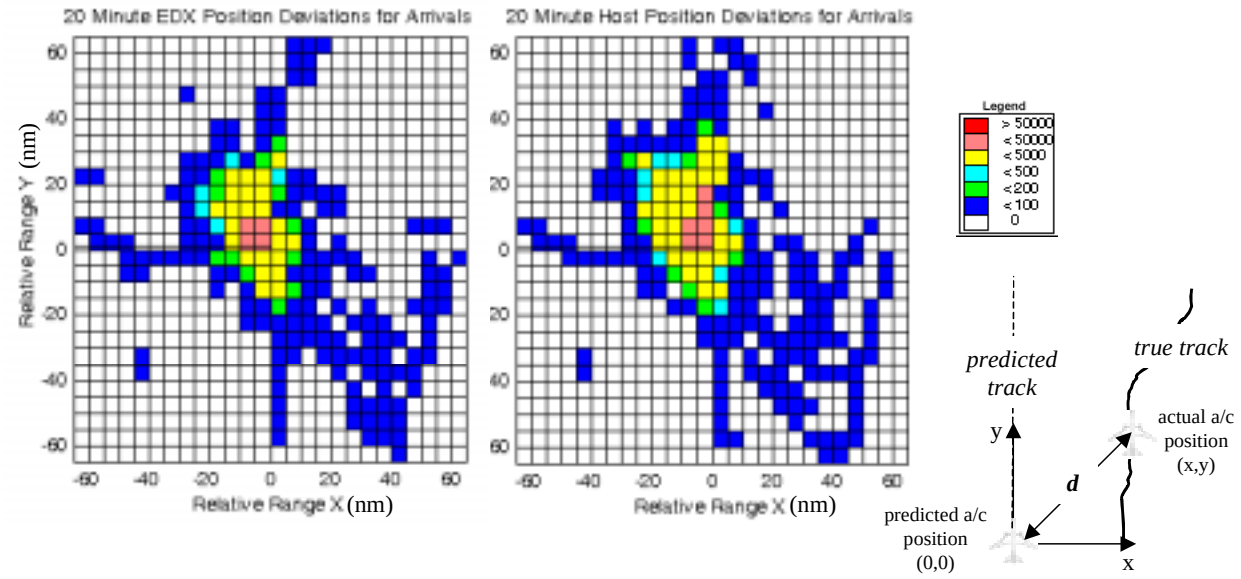

Figure 21 Sample Predicted Position Scatterplot Diagrams

Then, a representative prediction error deviation due to intent, σ_i, was determined for both EDX and Host data cases for lookahead times ranging from 5 to 30 minutes. For a given lookahead time and data case, σ_i was calculated by first determining the two-dimensional mean and standard deviation values: $\bar{x}$, $\bar{y}$, σ_x, and σ_y, respectively. Then, we assumed $\bar{x}, \bar{y} = 0$ over large numbers of aircraft trials because of no known biasing phenomena (and, in the case of a consistent bias error, a good conflict probe would seek to improve its predictive model to take out such a bias). Finally, we calculated a representative σ_i assuming that the predicted position variances were composed of non-correlated x and y -based position variances, such that $\sigma_i^2 = \sigma_x^2 + \sigma_y^2$ (for a citation of a similar calculation for a horizontal 2D standard deviation quality measures for GPS position accuracy, see [17]). The determined σ_i for Arrivals, Departures, Overflights, and all aircraft, for both EDX and Host data cases, are shown in Figure 22. Note: at $\tau = 0$, there is no prediction error and, therefore, $\sigma_i = 0$.

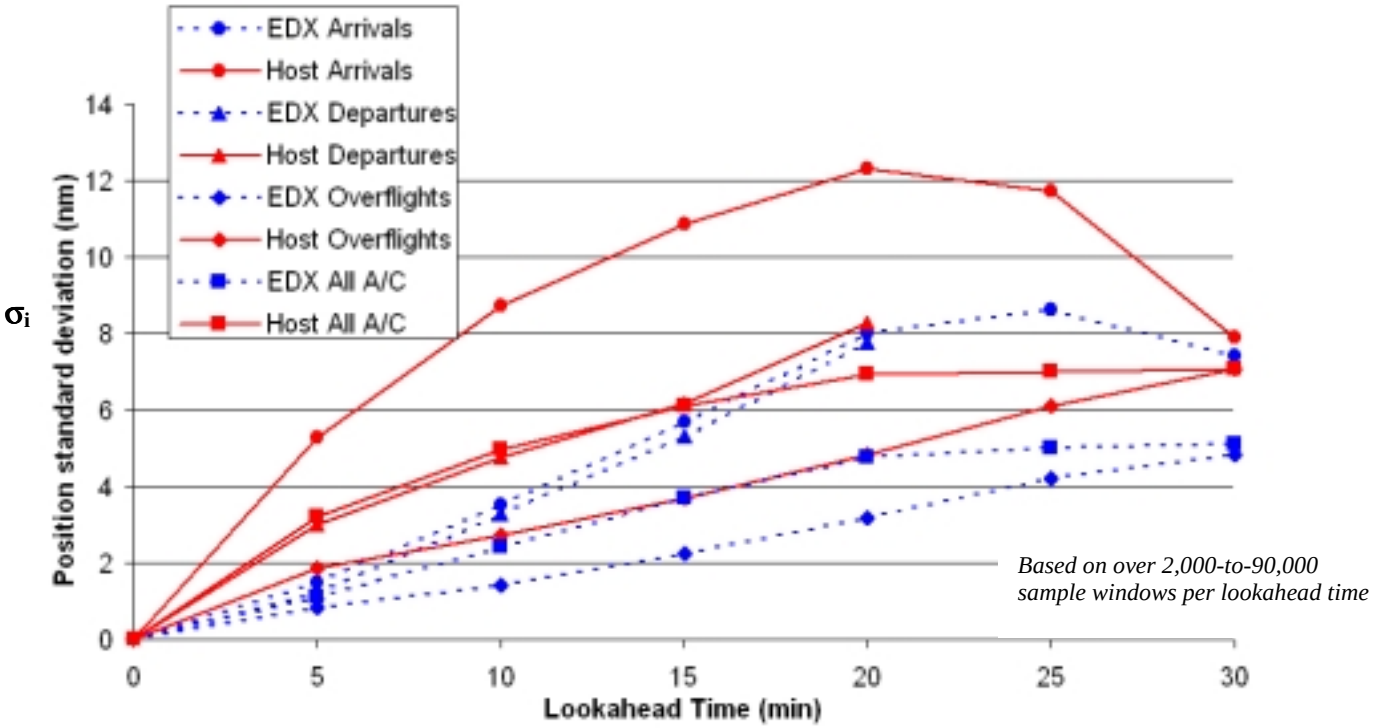

Figure 22 EDX and Host-based Predicted Position Error as a Function of Lookahead Time

Key Finding: Intent-based predicted position error is strongly affected by lookahead time, phase of flight, and source of intent data. Figure 22 illustrates that arrivals exhibit a maximum intent-based predicted position error at 20 minute lookahead times, while overflights exhibit increasing errors beyond 30 minute lookahead times. The primary reason for this is expected to be the natural convergence of potential arrival routes at larger lookahead times.

Key Finding: Potential reduction in intent-based predicted position error due to is a function of lookahead time and phase of flight As we expected, the downlinked EDX waypoint information provides significant reductions in predicted position error over that found in predictions based on Host flight plans. However the potential reduction in predicted position error due to use of EDX data is a function of both lookahead time and phase of flight. The greatest reductions in intent-based predicted position error occur for the arrival phase of flight for moderate lookahead times of 10 to 20 minutes. The arrival phase of flight was expected to provide the most fruitful opportunity for EDX improvement because of the already noted greatest Host Lateral Intent errors (see Figure 8 in Section 3.2). The moderate lookahead times for Arrivals offer the greatest potential benefit (i.e., greatest $\sigma_i\big|_{Host} - \sigma_i\big|_{EDX}$) because they are the lookahead times where the Active and Active+1 waypoints are valid. Beyond Active+1 waypoints, the EDX predicted intent reverts back towards that of the Host predicted intent. Overall, the Arrival σ_i increases up to 20 minutes lookahead and then decreases. This occurs because of the convergence of potential Arrival routes for larger lookahead times.

Departures exhibit values of σ_i less than Arrivals, but greater than Overflights and an overall potential reduction in predicted position error that peaks at 5 minutes lookahead. Note: that

values of σ_i for lookahead times of 25 and 30 minutes were deemed statistically insignificant given the total numbers of sample windows were 350 and 31, respectively.

Overflights exhibit a steadily increasing σ_i, but a slowly growing potential reduction in predicted position error that are greatest at the furthest lookahead time. This is primarily because of the large typical lookahead times for Overflight Active and Active+1 waypoints (see Figure 12 in Section 3.2).

When averaging σ_i over all valid flights, we obtain significant reductions in σ_i throughout the "All" lookahead times.

Having convinced ourselves that downlinked EDX position, ground speed, and intent data are likely to improve our conflict probe performance, the key question is *By how much?*

Conflict Detection Performance Analysis Methodology and Results

A number of previous analytical and real-time conflict probe-based analyses of stochastic conflict detection performance have been performed [18][19][20][21][22]. A comprehensive conflict probe assessment similar to [22] using ATM conflict probe automation with and without downlink data code modifications is probably the most effective way to quantify conflict probe improvements, but, for the purposes of the current effort, time prohibitive. However, an alternative method to determine order of magnitude impacts on conflict probe performance was developed and implemented and is now explained.

For the purposes of simplicity, a two-dimensional conflict test case was posed. This test case consisted of two jet aircraft with a 90 deg crossing conflict at an arbitrary initial range and bearing from each other. Both aircraft are flying level in en route airspace at a constant ground speed of 450 kts with no wind. A conflict probe is predicting the aircraft conflict using a flight-plan-based intent model for each aircraft. The flight plan-based predicted track is off of the true track in a statistically similar way to that analyzed in Section 3.2. No traffic flow management constraints are active. The initial conditions are shown in Figure 23 and Figure 24 in the inertial and Aircraft A-relative reference frames, respectively.

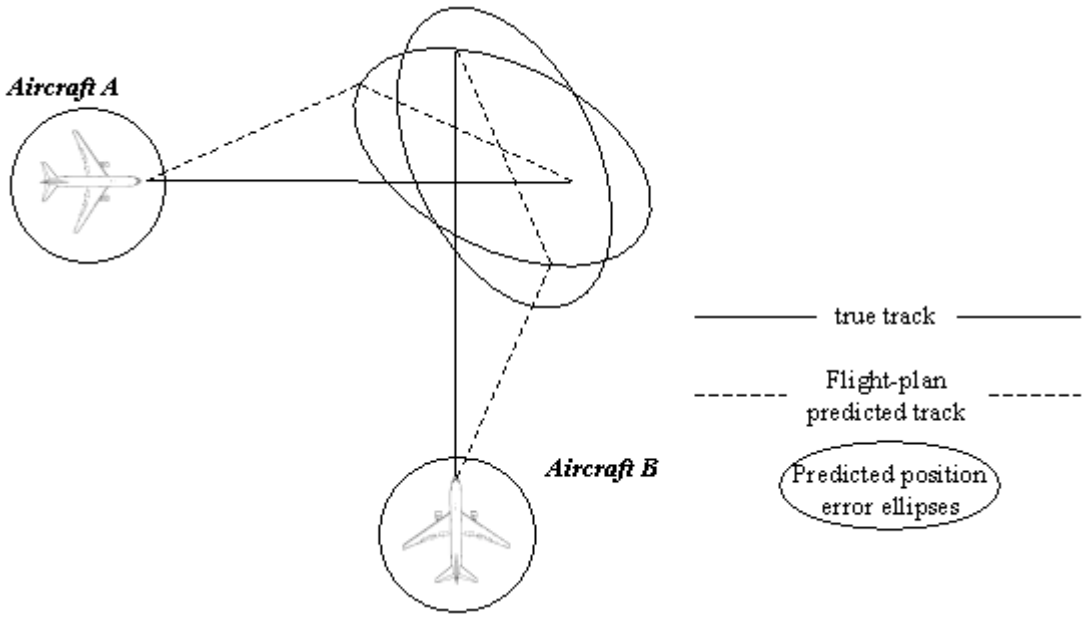

Figure 23 Conflict Detection Test Case: Inertial Reference Frame

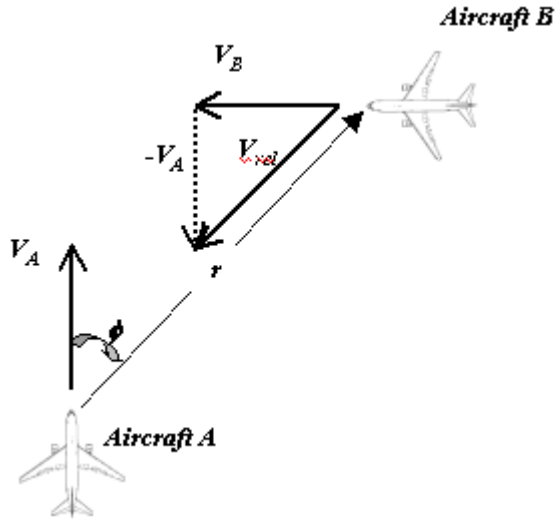

Figure 24 Conflict Detection Test Case: Aircraft A-Relative Reference Frame Geometry

Now, we will assume that the predicted position error for a given aircraft at a future time, τ, can be represented by the expression, $\sigma_{p,p}$. Assuming that this predicted position error can be decomposed into independent, Gaussian, random, predicted position errors due to current position, current velocity, and intent, σ_p, σ_v, and σ_i respectively, we can derive the expression:

$$\sigma_{p,p}{}^2(\tau) = \sigma_p{}^2 + \tau^2\sigma_v{}^2 + \sigma_i{}^2 \qquad (3.4.1)$$

Taking the values for GPS and radar-derived σ_p, σ_v and σ_i previously derived from Figure 19 and Figure 22 for values of lookahead time between 0 and 30 minutes, we can calculate $\sigma_{p,p}{}^2$. The results for Arrivals and Overflights are plotted in Figure 25 and Figure 26.

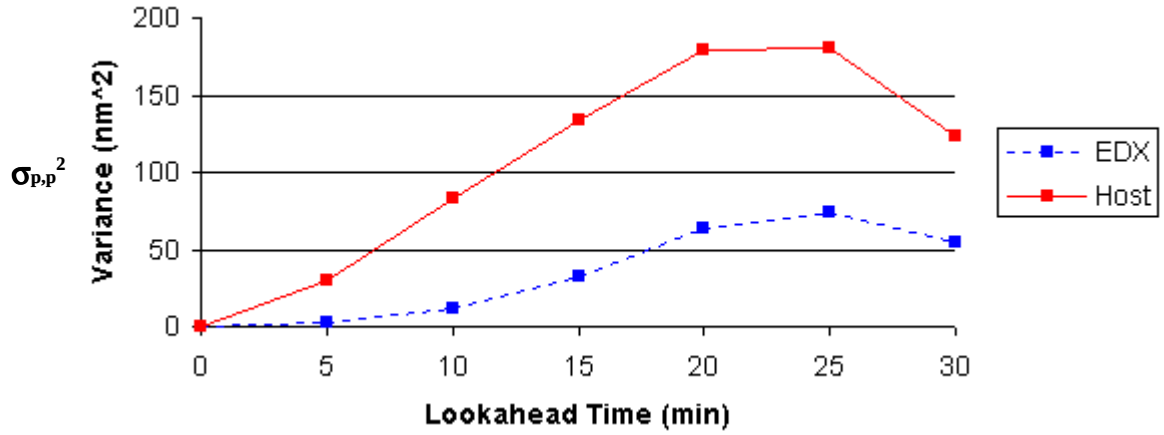

Figure 25 EDX and Host-derived Predicted Position Variances: Arrivals

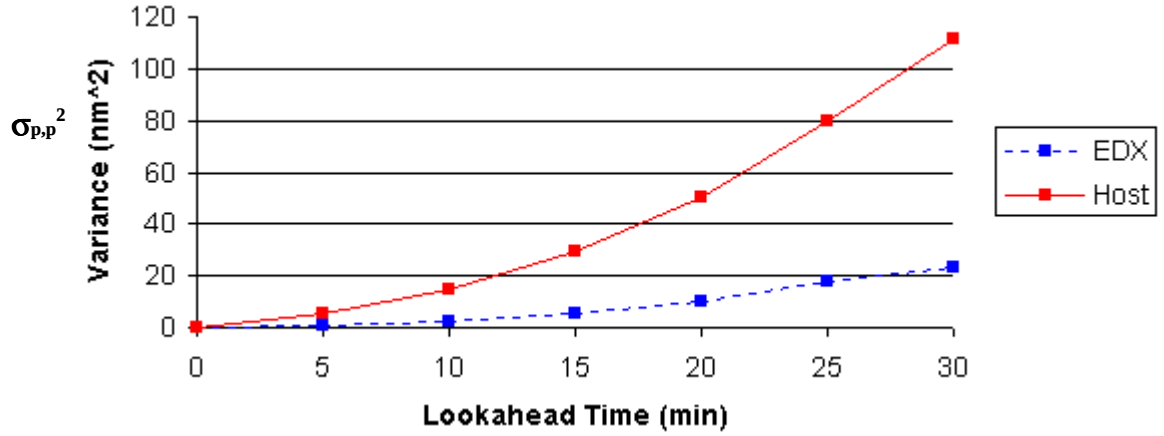

Figure 26 EDX and Host-derived Predicted Position Variances: Overflights

As Figure 25 and Figure 26 show and as we expected, the predicted position variance due to the EDX data is significantly less than that for the Host data for the full range of lookahead times from 5 to 30 minutes. The characteristics of the curves are similar to that derived in Figure 22 for determining σ_i. In the case of Arrivals, the both EDX and Host variances show a maximum variance in the 25 minute lookahead time region. The maximum reduction in predicted position variance for the EDX was achieved for a 20 minute lookahead time and the use of EDX data resulted in a predicted position variance roughly 1/3 that using Host data. In the case of Overflights, both the EDX and Host variances show a maximum variance at the edge of the investigated lookahead time window at 30 minutes. The maximum reduction in predicted

position variance for the EDX was achieved for the 30 minute lookahead time and the use of EDX data resulted in a predicted position variance roughly 1/5 that using Host data.

An investigation into the relative magnitudes of the components of the predicted position variance from Equation 3.4.1 (i.e., that due to current position, current velocity, and predicted intent) for both EDX and Host data cases yields interesting results. The individual variances of the 3 components for both EDX and Host data in both Arrival and Overflight cases were calculated and are shown in Figure 27 and Figure 28.

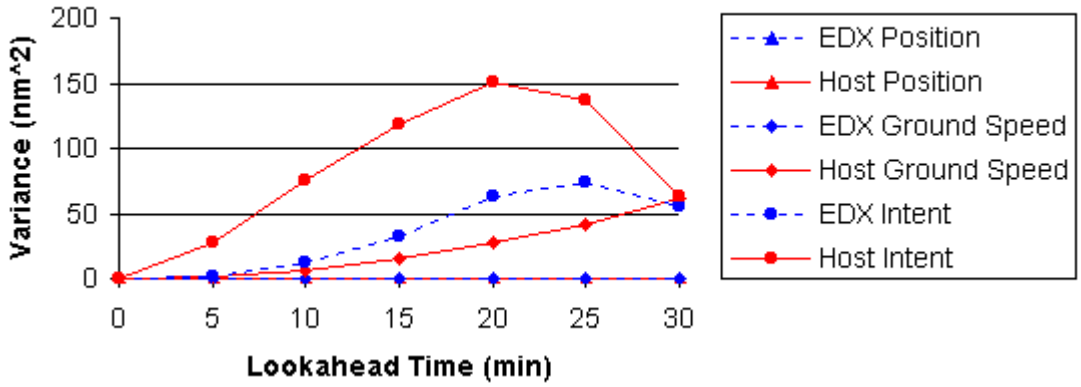

Figure 27 EDX and Host-derived Predicted Position Component Variances: Arrivals

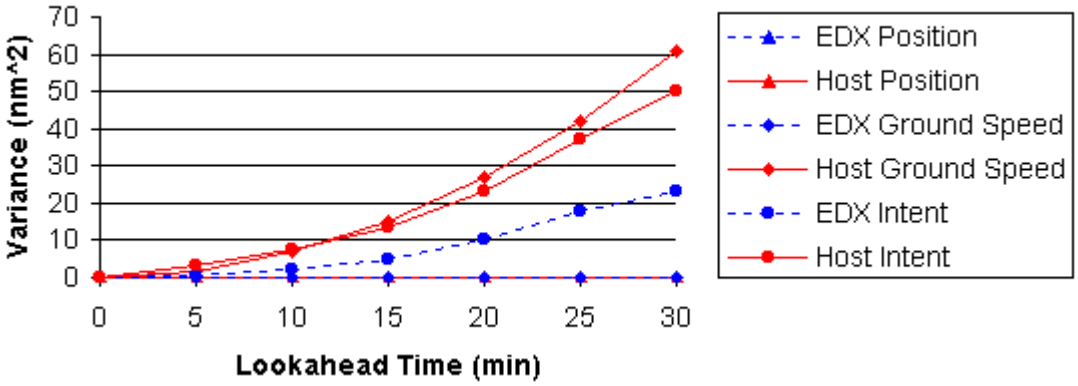

Figure 28 EDX and Host-derived Predicted Position Component Variances: Overflights

Key Finding: In terms of contributing to overall predicted position variance, the overwhelmingly important components are intent and current velocity. The results of Figure 27 and Figure 28 show that, for Arrivals, significant intent errors dominate the variance of predicted future positions up to 20 minute lookahead times. Velocity errors dominate the variance of predicted future positions for both longer lookahead times for Arrivals and generally for all non-Arrivals. In both EDX and Host data cases, current position errors are negligible, and, in the EDX case, the current velocity error is negligible as well.

In the case of Arrivals, intent errors dominate the variance over the 5-to-30 minute lookahead times, but begin to yield to quadratic lookahead time dependency of the current velocity variance component at the upper boundary of lookahead times. Similarly, the reduction of total predicted position variance due to the EDX data is predominantly due to improved intent predictions for all lookahead times, except for those in the upper 30 minute lookahead region. In the case of Overflights, the lower levels of intent errors experienced (see Figure 8 and Figure 10 in Section 3.2) enable the domination of the current velocity variance component to dominate the variance for lookahead times equal to and greater than 15 minutes. Similarly, the reduction of total predicted position variance due to the EDX data is predominantly due to improved current velocity information for lookahead times equal to and greater than 10 minutes.

Next, Equation (3.4.2), derived in previous research [21], describes the variation in aircraft conflict miss distance as a function of the predicted trajectory position accuracy at the point of closest approach for Aircraft A and B:

$$\sigma_{r_f} = \sqrt{\sigma_{p,p,A}{}^2 + \sigma_{p,p,B}{}^2} \tag{3.4.2}$$

Assuming that the predicted position error for each aircraft will be the same, we ultimately derive:

$$\sigma_{r_f} = \sigma_{p,p}\sqrt{2} \tag{3.4.3}$$

In previous Seagull conflict probe analysis research [18], the probability of conflict for a 2D, two aircraft conflict was analytically derived as:

$$P(conflict) = \frac{1}{2} erf\left(\frac{R + r_f}{\sqrt{2}\sigma_{r_f}}\right) + \frac{1}{2} erf\left(\frac{R - r_f}{\sqrt{2}\sigma_{r_f}}\right) \tag{3.4.4}$$

where:

R is the Protected Airspace Zone (PAZ) radius,

r_f is the separation at the closest point of approach (CPA), and

σ_{r_f} is the one sigma minimum separation error.

Equation (3.4.4) can, in turn, be used to determine the probability of conflict for our test case for arbitrary initial relative distance and bearing (of Aircraft B from Aircraft A). These conflict probabilities can then be plotted in the relative Aircraft A reference frame, thus creating a "conflict probability map" (similar to what has been done previously in [18]).

For the theoretical case of perfect current and future knowledge of aircraft states (i.e., $\sigma_p = \sigma_v = \sigma_i = 0$), the conflict probability map would look like Figure 29. In this case, any intruder aircraft initial conditions within the shaded region (Region I) would yield

P(conflict)=1.0 (i.e., 100% probability of correctly identifying the conflict) and those outside of the shaded region (Region II) would yield P(conflict)=0.0. In this special case, the P(false alarm)=P(missed alerts)=0 and P(correct alerts)=1.0. Note: we assume that "correct alerts" consist of both an *alert* if the intruder aircraft eventually violates the Protected Airspace Zone or *no alert* if there is no such eventual violation.

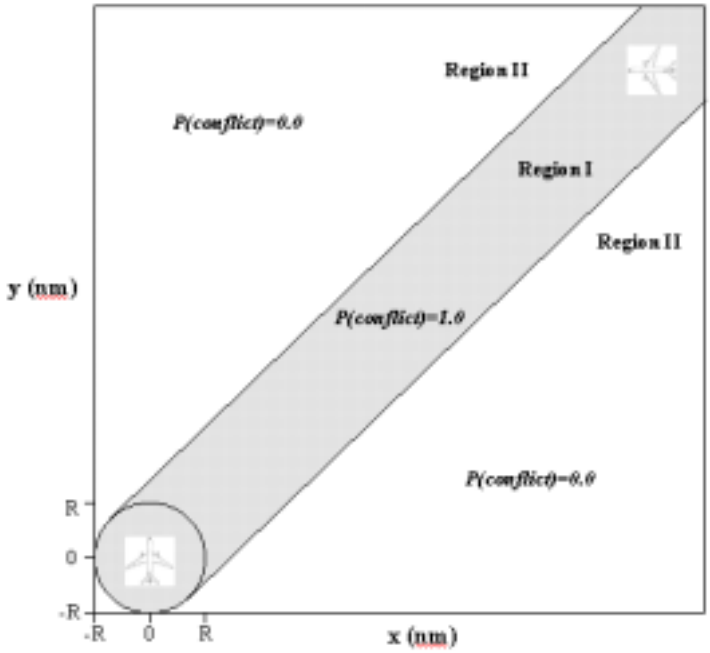

Figure 29 Conflict Prediction Probability Map assuming Perfect Knowledge

In the practical case of imperfect current and future knowledge of aircraft states (i.e., $\sigma_p, \sigma_v, \sigma_i > 0$), the conflict probability map will look like Figure 30.

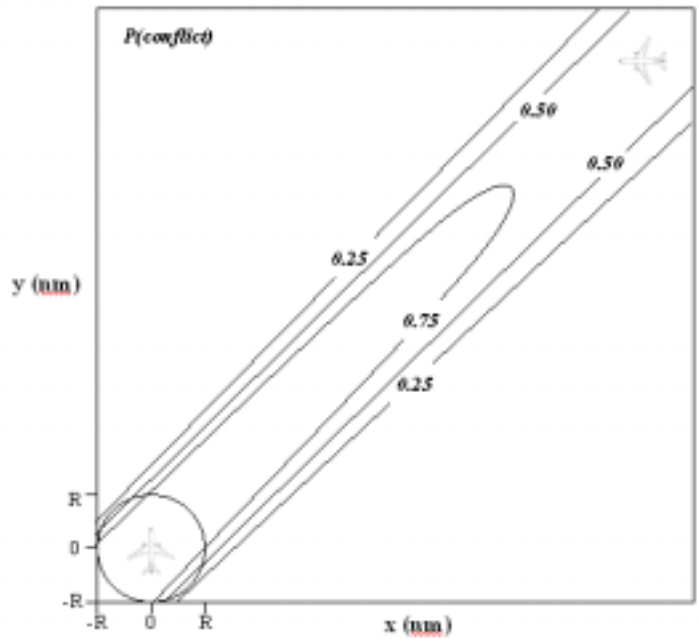

Figure 30 Conflict Prediction Probability Map assuming Imperfect Knowledge

In this case, any aircraft initial conditions will yield P(conflict)<1.0 and the probability map will yield a contour plot of conflict probabilities with P(conflict) getting smaller with distance from the Protected Airspace Zone. In the imperfect case, P(false alarm), P(missed alerts), and P(correct alerts) are between 1.0 and 0.0. Then, depending on the given initial conditions, either P(correct alerts) + P(missed alerts) = 0 (in the case of an eventual violation of the Protected Airspace Zone, i.e., with the intruder aircraft's initial conditions in Region I of Figure 29) or P(correct alerts) + P(false alarms) = 0 (in the case of an eventual non-violation of the Protected Airspace Zone, i.e., with the intruder aircraft's initial conditions in Region II of Figure 29). Note: the additional issues of "perceived" conflicts and acceptable controller spacing are not addressed here, but are dealt with extensively in [21] and recommended for the interested reader.

The impact of reduced sensing and prediction errors due to improved technology in sensing aircraft state or determining intent (e.g., EDX data downlinks) will impact the conflict probability map. Improved technology will push the given "current technology" conflict probability contours (e.g., such as that shown in Figure 30) further out in time and sharpen the gradient where the contours intersect the PAZ. Thus, the impact of the improved technology will result in a new conflict probability map that will be closer to the "perfect case" shown in Figure 29.

Going back to our conflict detection test case to quantify the expected impacts of EDX downlinked data on conflict detection performance, we first assume a value of 5 nm for R, the diameter of the PAZ, which equals the nominal en route US airspace separation standard. Then, we calculate σ_{r_f} from Equation (3.4.3) and the data in Figure 25 and Figure 26. Finally, we determine r_f based on conflict geometry, and we use Equation (3.4.4) to derive a conflict probability map for a given set of initial r, ϕ initial conditions and for either EDX or Host Data

cases. Conflict probability maps for EDX and Host data cases were developed for the Arrival data and are shown in Figure 31. In order to better understand the relative impact of EDX data, the two conflict probability maps were differenced and are shown in Figure 32 (i.e., P(conflict) of Figure 32 = P(conflict) of Figure 31a using EDX data - P(conflict) of Figure 31b). Analogously, the conflict probability maps for Overflights were developed and are shown in Figure 33 and Figure 34.

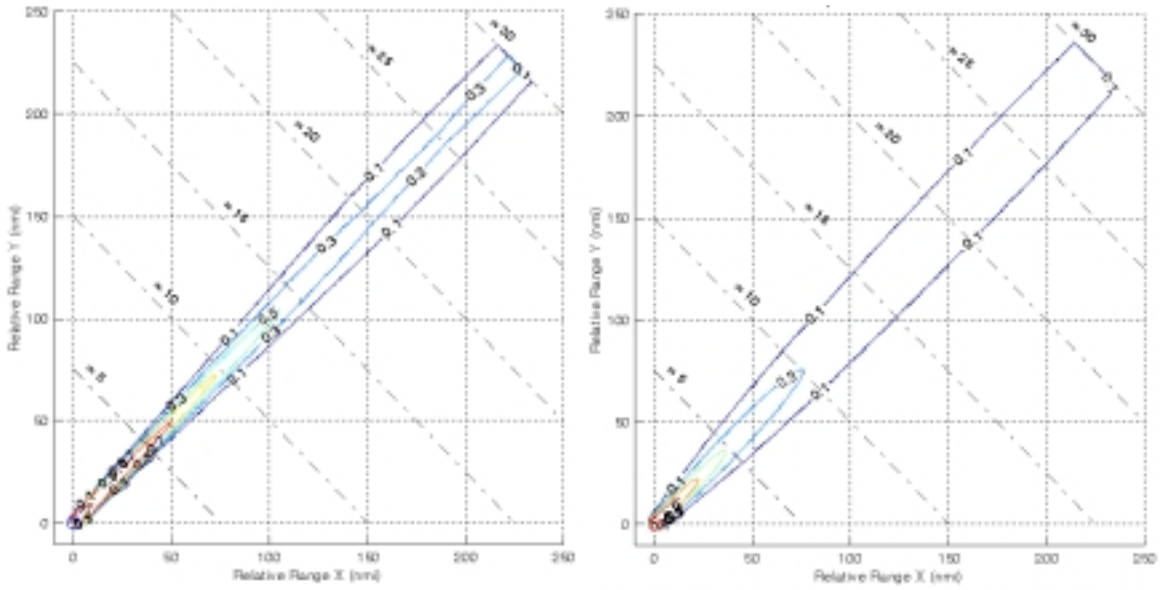

a) EDX Data **b) Host Data**

Figure 31 Conflict Probability Maps for EDX and Host-based data: Arrivals

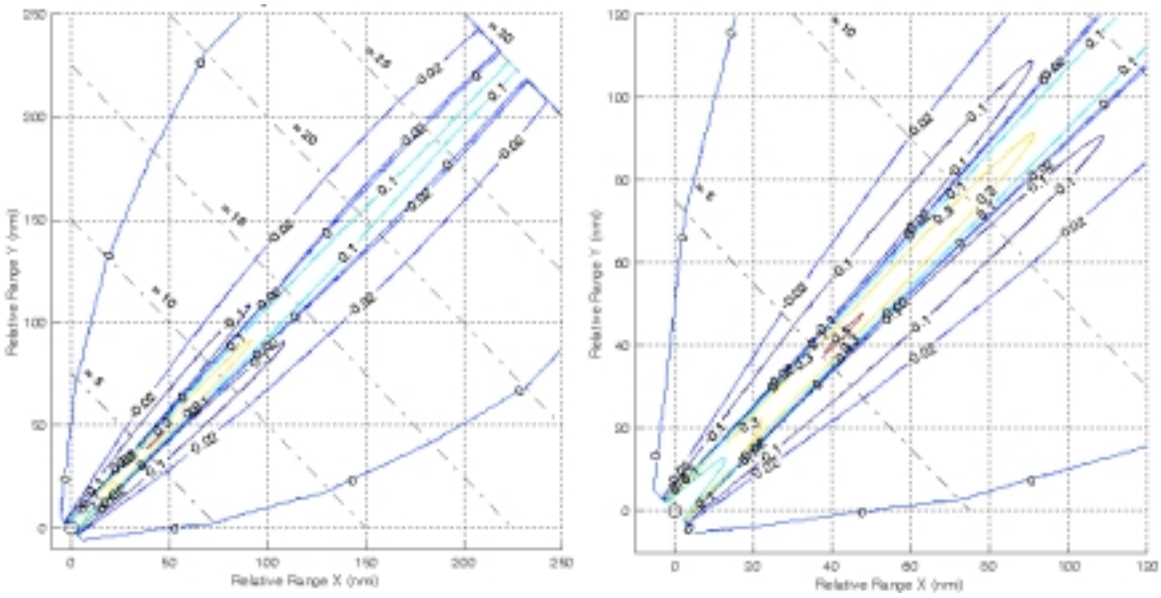

a) Overview **b) Zoom-In**

Figure 32 Differenced EDX-Radar Conflict Probability Map: Arrivals

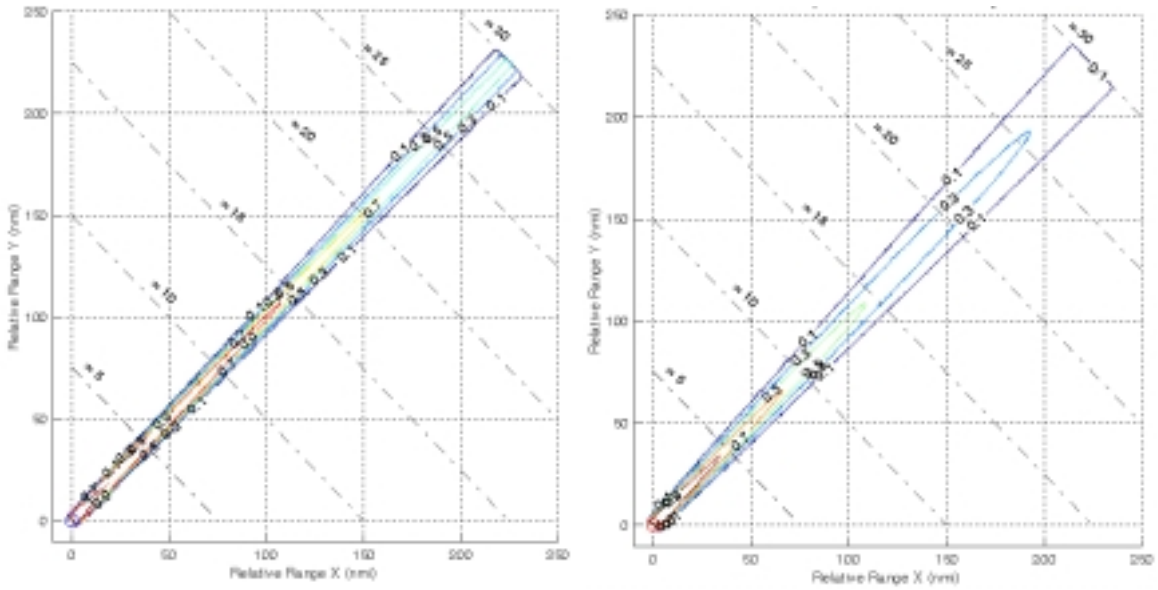

a) EDX Data **b) Host Data**

Figure 33 Conflict Probability Maps for EDX and Host-based data: Overflights

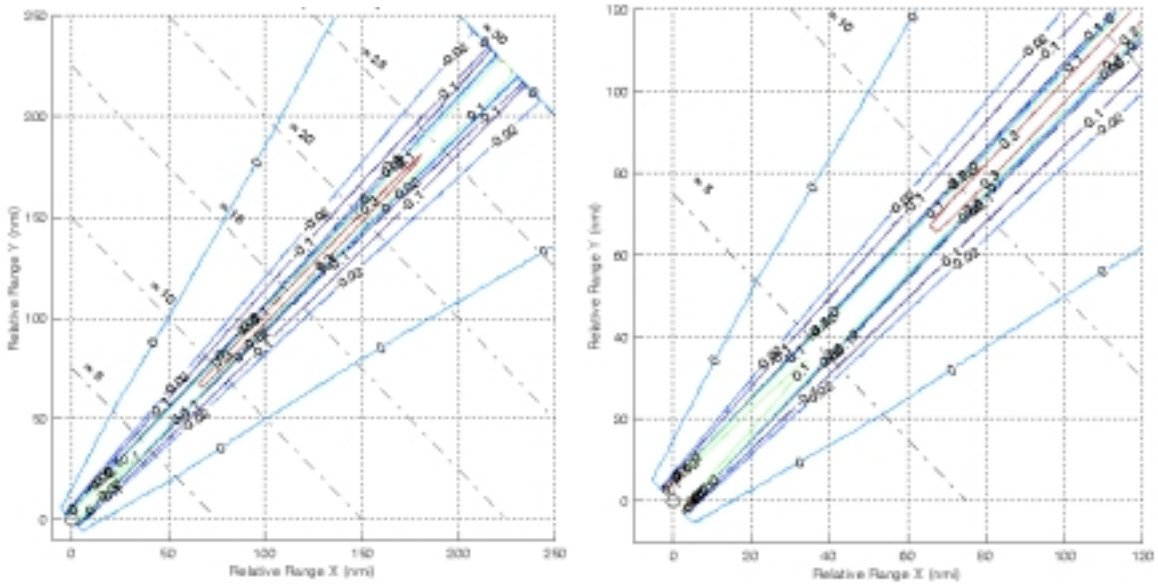

a) Overview **b) Zoom-In**

Figure 34 Differenced EDX-Radar Conflict Probability Map: Overflights

The conflict probability maps in Figure 31 and Figure 33 display what we expected: isoprobability lines that extend further out in time and wrap more tightly around the PAZ for predictions using the higher precision EDX data. The differenced conflict probability maps in Figure 32 and Figure 34 show the general trend of positive probability differences along the

conflict centerlines and pockets of negative probability differences just outside the extended 45 degree lines from the PAZ. These differences can be interpreted as quantitative EDX-based reductions in conflict probe missed alert and false alarm rates as follows.

Examining a typical differenced conflict probability map, Figure 35 we see two important cases. In the first case, aircraft A will be in conflict with aircraft B' (i.e., aircraft B' is in Region I of Figure 29. In the second case, aircraft A is not going to be in conflict with aircraft B'', but will miss aircraft A's PAZ by not very much (i.e., in Region II of Figure 29), but close to the Region I-Region II interface). Taking the conflicting case first, let's assume the predicted probability of conflict of aircraft A with aircraft B' using Host data, P(Host-based conflict), = 0.50 for a lookahead time τ'. Since, based on its initial position, we know that aircraft A and B' will be in conflict, the fact that P(Host-based conflict) = 0.50, means that for our given initial lookahead time, τ', P(correct alert)= P(Host-based conflict)=0.50. This also means that P(missed alert)=1-P(correct alert) = 0.50. In other words, there is a 50% chance of a missed alert. Now, looking again at Figure 35, we notice that since aircraft B' is in the red, diagonally-crosshatched zone, the predicted probability of conflict of aircraft A with aircraft B' using EDX data is 0.3 (=δ) greater than the predicted probability of conflict of aircraft A with aircraft B' using Host data. This means that P(EDX-based conflict) = P(Host-based conflict) + δ = 0.5 + 0.3. Therefore P(correct alert) using the EDX data is greater than P(correct alert) using the Host data by δ, and, likewise, the P(missed alert) using the EDX data is less than P(missed alert) using the Host data by δ.

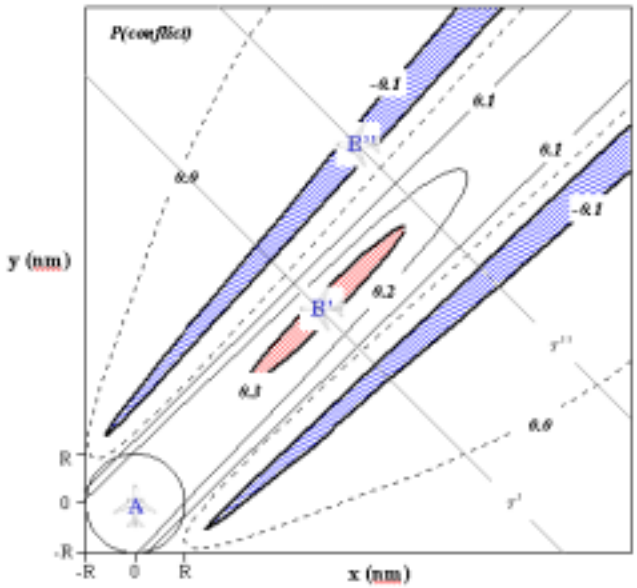

Figure 35 Typical Differenced EDX-Radar Conflict Probability Map

A similar analysis can be done for the non-conflict between aircraft A and aircraft B'' to show that P(false alarm) using the EDX data is less than the P(false alarm) using the Host data by - δ. Therefore, in cases of a non-conflicting test case with aircraft B'' initial conditions in Region II and δ<0, the false alarm rate is reduced by the absolute value of δ.

Thus, the difference statistics in Figure 32 and Figure 34 provide a map for expected missed alert and false alarm impacts of EDX downlink data for all relative aircraft initial conditions.

Key Finding: Downlinked FMS data are expected to significantly reduce missed detection and false alarm and alert rates of current technology conflict probes. Close inspection of the Figure 32 and Figure 34 plots reveal the order-of-magnitude missed alert and false alarm impact statistics for our crossing conflict probe test case and are shown in Figure 36.

	Missed Alert Rate Impact	*False Alarm Rate Impact*
Arrivals	At 6 minutes lookahead time for a crossing collision, missed alert rates drop a maximum of 50%. Longer lookahead times result in smaller missed alert rate reductions approaching 10%.	For lookahead times between 0 and 13 minutes for "near-conflicts" with minimum separation distances roughly 2*PAZ diameter, false alarm rates drop a maximum of 10+%.
Overflights	At 8 to 24 minute lookahead times for a crossing collision, missed alert rates drop a maximum of 30+%.	For lookahead times from 0 to 30 minutes and "near-conflicts" with minimum separation distances roughly sqrt(2)*PAZ diameter, false alarm rates drop 10+%.

Figure 36 Order of Magnitude EDX Missed Alert and False Alarm Rate Impacts

For the analysis conducted, missed alert rate reductions can be as high as 50% in the case of arrivals and can provide 30+% reductions for overflights. False alarm rate reductions are lower than the missed alert rate reductions, and are expected to decrease 10+% or less. Specific reductions in missed detection and false alarm rates will vary based conflict initial conditions, the specific position, velocity, and intent errors experienced, and other factors not accounted for (such as wind prediction errors).

The previous conflict detection analysis resulted in the development and implementation of an 2D order-of-magnitude analysis methodology that took FMS and radar-based position, velocity, and intent data and predicted order-of-magnitude impact of state and intent-sensing technology improvements on conflict prediction probabilities and missed alert and false alarm rates. In the future, this analysis could be extended to look at other conflict scenarios such as arrival merging or overtaking conflict cases. Also, the impact of controller conflict buffers (also known as "acceptable controller spacing" (ACS)) can be taken into account leveraging the methodology of [21]. However, future attempts to examine the impacts of downlinked EDX on conflict probes, would be wise to leverage the real-world use of a conflict probe decision support tool (modified to incorporate either radar-based or EDX-based data) in a manner consistent with [22].

4 Conclusions and Recommendations

4.1 General Conclusions

The results of this study suggest that substantial benefits can be achieved by the delivery of aircraft parameters to ATC over real-time data link. In particular, the downlink of FMS aircraft state variables and particularly the FMS intent can greatly improve ATC trajectory prediction accuracy in enroute and transition airspace. Accurate trajectory predictions are crucial for maximizing the performance, benefits, and controller acceptance of ATC decision-support tools such as CTAS.

Based on the collection of real-world operational data, the results of this study showed that:

1) sizable errors are associated with existing ATC data sources, and
2) significant improvement in ATC decision support tool trajectory prediction accuracy are enabled with the incorporation of downlinked aircraft data.

Finally, as an important engineering achievement, this study proved that a wealth of aircraft data could be extracted with minimal avionics intrusion and with minimal transit delay.

4.2 Summary of Key Findings

A number of key findings were identified throughout this report, and are summarized below, along with a reference to the section where the findings are supported by the data and analysis.

1. Even with minimal engineering modifications and using the existing ACARS datalink (which was not specifically designed to meet the EDX vision), a wealth of aircraft data can be extracted with minimal avionics intrusion and transmitted reliably to ATC with minimal transit delay (Section 3.1). Over an eight-month period, data were collected for over 1,000 operations within Denver ARTCC airspace. For 60 randomly selected flights, the average message delay was found to be 9 sec with a standard deviation of 12 sec. In processing the data using automatic "scripts," we found the data to be of high integrity, with instances of missing or unintelligible data being extremely rare.

2. EDX downlink of aircraft sensor and flight intent data can significantly reduce trajectory prediction errors for decision support tools (Section 3.1). Large deviations were found between Host radar measurements of the aircraft state variables and the corresponding downlinked parameters. Particularly significant were deviations in the aircraft weight and flight intent.

3. FMS lateral intent was often ambiguous in the data owing to the specific design choices of the downlink process, but ambiguities could be largely resolved through post processing (Section 3.2). In the original planning, it was decided to use only four characters to represent waypoints, leading to ambiguities. We recommend that future implementations of FMS intent downlink use a 5-character representation for the waypoint name and continue to downlink next-waypoint range/bearing to further enhance data integrity. Further, we point

out that it is important to synchronize the onboard and ground waypoint databases, again to ensure data integrity.

4. Downlinked FMS intent significantly reduces the average and maximum lateral intent error for Arrivals, Departures and Overflights (Section 3.2). For Arrivals, the reduction in the average lateral route intent error is considerable – a reduction from over 6 nmi to 1.72 nmi. The averages are reduced considerable in the Departures and Overflights categories as well.

5. A significant population of flights exhibit a mean Host Lateral Intent Error (HLRIE) greater than 4 nmi (Section 3.2). Over 54% of the Arrivals exhibited mean HLRIE values greater than 4 nmi. Correspondingly, 25% of the Departures and only 4% of the Overflights showed a mean HLRIE greater than 4 nmi. A large population of Arrivals had HLRIE values in the 12 to 18 nmi range.

6. Downlinked FMS Intent greatly reduces the population of flights exhibiting mean Lateral Intent Errors greater than 4 nmi (Section 3.2). The number of Arrivals exhibiting mean FLRIE values greater than 4 nmi is reduced to 13% of the 191 population (compared to 54% for the HLRIE). For Departures, the mean FLRIE was reduced also to 13% of the 166 population (as compared to 25% HLRIE) and none of the Overflights showed a mean FLRIE over 4 nmi (as compared to 4% HLRIE).

7. For Arrivals, the average look-ahead time represented by downlinked FMS Active and Active+1 waypoints was 13.2 minutes; for Departures and Overflights the corresponding average look-ahead times were 33.5 and 37.5 minutes, respectively (Section 3.2). Fifty-one (51) of the 191 Arrivals (27%) exhibit an average look-ahead time of less than 10 minutes, and the largest population of Arrivals exhibit 15 to 20 minutes of FMS intent look-ahead. Only 30 Departures out of the 166 population (18%) exhibit average look-ahead times less than 20 minutes. The rest of the Departures and all the Overflights, on average, are covered by more than 30 minutes of flight by downlink of only two FMS waypoints.

8. EDX downlink of FMS weight and flight intent parameters greatly improve the ability of decision support tools to predict the altitude profiles and lateral trajectory of the aircraft, as compared to radar truth (Section 3.3). Downlink of EDX weight data alone improved the accuracy of predicted altitude by an average of nearly 30%. The use of both EDX weight and speed intent improved altitude and path distance predictions by an average of 53% and 24%, respectively. For a 20-flight sample, lateral path prediction accuracy was improved by 60% with the use of EDX route intent data, provided in the form of FMS waypoints.

9. Potential reduction in intent-based predicted position error due to is a function of lookahead time and phase of flight (Section 3.4) The greatest reductions in intent-based predicted position error occur for the Arrival phase of flight for moderate lookahead times of 10 to 20 minutes. Additionally, Arrival intent-based predicted position error increases up to 20 minutes lookahead and then decreases. This occurs because of the convergence of potential Arrival routes for larger lookahead times. Overflights exhibit a slowly growing potential reduction in predicted position error that are greatest at the furthest, 30 minute lookahead

time. This is primarily because of the large typical lookahead times for Overflight Active and Active+1 waypoints.

10. In terms of contributing to overall predicted position variance, the overwhelmingly important components are intent and current velocity (Section 3.4). For Arrivals, significant intent errors dominate the variance of predicted future positions up to 20 minute lookahead times. Velocity errors dominate the variance of predicted future positions for both longer lookahead times for Arrivals and generally for all non-Arrivals. In both EDX and Host data cases, the impact of current position errors are negligible, and, in the EDX case, the current velocity error is negligible as well.

11. Downlinked FMS data are expected to significantly reduce missed detection and false alarm and alert rates of current technology conflict probes (Section 3.4). For the analysis conducted, missed alert rate reductions can be as high as 50% in the case of arrivals and can provide 30+% reductions for overflights. False alarm rate reductions are lower than the missed alert rate reductions, and are expected to decrease 10+% or less. Specific reductions in missed detection and false alarm rates will vary based conflict initial conditions, the specific position, velocity, and intent errors experienced, and other factors not accounted for (such as wind prediction errors).

4.3 Recommendations for Future Work

The EDX Project has established a valuable asset in the EDX Laboratory and collected a body of flight data. The potential exists to continue data collection activities so as to amass a statistically significant amount of downlink FMS data to support new and on-going efforts aimed at developing data requirements and establishing benefits for next-generation data link systems and services. Such planned and current efforts are intended to explore concepts that further integrate ground-based decision support tools with flight deck information systems, for the benefit of controllers and airspace users alike.

To date, essentially all data analysis results have been obtained through post-processing, due to difficulties in establishing the real-time version of EDX CTAS. It is recommended that the real-time EDX CTAS variant be completed and validated in the EDX Laboratory. In accomplishing this work, we recommend that a real-time work-around be devised for resolving ambiguities in the downlinked FMS Active and Active+1 waypoint data. Establishing the real-time EDX CTAS will enable side-by-side performance comparisons between the Baseline CTAS and the improved version that exploits FMS downlinked data. The comparable real-time versions will also enable human-machine interface (HMI) studies related to the benefits of data exchange.

The results presented here suggest that significant benefits could be obtained in trajectory predictions and subsequent ATC advisories arising from specific ATM automation incorporation of live, downlinked EDX data. Some of the ATM decision support tools that could benefit include CTAS' Direct-To, Conflict Probe, Traffic Management Advisor, and En Route Descent Advisor automation and MITRE's User Request Evaluation Tool (URET). Future work should aim at validating the potential benefits through comparison of the performance of these specific ATM automation tools with and without the data exchange.

The quantitative results from the recommended continued research of this section are expected to and should provide data to augment previous FAA and NASA benefits analyses of potential user fuel and time savings due to user-ATM data exchanges [23][24]. Previous studies have made assumptions on the accuracy of various data inputs, both with and without user-ATM data exchange. The continued EDX Phase 2 field evaluation research will provide more accurate values for these parameters, which can be used to fine-tune and verify the potential benefits estimates resulting from these studies.

The beneficial impacts of the downlinked EDX data performed in this effort are just the dawn of a new era in planned ATM service improvements leveraging the addressed data link. Recently released reference [25] details many new one-way and two-way data link-enabled ATM services envisioned for all flight domains. Future analyses such as the one performed in this effort will need to be performed to predict and validate the potential impacts of the new data link-enabled ATM services.

Glossary

2D	Two-dimensional
3D	Three-dimensional
4D	Four-dimensional
ACARS	Aircraft Communications Addressing and Reporting System
ACS	Acceptable Controller Spacing
ADL	FAA's Aeronautical Data Link Product Team
ADNS	ACARS Data Network System
AOC	Airline Operational Control
ARINC	Aeronautical Radio, Inc.
ARSR	Air Route Surveillance Radar
ARTCC	Air Route Traffic Control Center
ATC	Air Traffic Control
ATM	Air Traffic Management
CAS	Calibrated Airspeed
CPA	Closest Point of Approach
CTAS	Center/TRACON Automation System
deg	degree
EDX	NASA's En Route Data Exchange Program
FAA	Federal Aviation Administration
FMS	Flight Management System
FLRIE	FMS Lateral Route Intent Error
GPS	Global Positioning System
Host CS	ARTCC Host Computer System
HLRIE	Host Lateral Route Intent Error
INS	Inertial Navigation System
kt, kts	knots
LNAV	Lateral Navigation
LRIE	Lateral Route Intent Error
m/s	meters per second
min	minutes

NAS	National Airspace System
NASA	National Aeronautics and Space Administration
nmi	Nautical miles
PAZ	Protected Airspace Zone
RMS	Root Mean Square
RUC	Rapid Update Cycle
STA	Scheduled Time of Arrival
TAS	True Air Speed
TRACON	Terminal Radar Approach Control
TS	Trajectory Synthesizer, a CTAS Software Process
UAL	United Airlines
URET	User Request Evaluation Tool
UTC	Universal Coordinated Time
VHF	Very High Frequency
VNAV	Vertical Navigation, a mode of the FMS that calculates a vertical trajectory profile
WAAS	Wide Area Augmentation System
ZDV	Denver ARTCC

References

[1] Erzberger, H., Davis, T.J., and Green, S.M., ”Design of Center-TRACON Automation System,” Proceedings of the AGARD Guidance and Control Panel 56th Symposium on Machine Intelligence in Air Traffic Management, Berlin, Germany, 1993, pp.11-1-11-12.

[2] Green, S.M., Goka, T., and Williams, D.H., “Enabling User Preferences through Data Exchange,” AIAA-97-3682, AIAA Guidance, Navigation, and Control Conference, August 1997.

[3] Weidner, T. and Mueller, T., “Benefits Assessment Compilation for En Route Data Exchange (EDX),” TM 00188.27-01, Seagull Technology, Inc., NASA TO27, December, 2000.

[4] Couluris, G.J., Weidner, T., and Sorensen, J., “Final Approach Enhancement and Descent Trajectory Negotiation Potential Benefits Analysis,” TM 97142-02, Seagull Technology, Inc., July 1997.

[5] Weidner, T., Davidson, T.G., “Fuel-Related Benefits Analysis of En Route Data Exchange,” TM 98175.9-01, Seagull Technology, Inc., December 1998.

[6] Schleicher, D., Weidner, T., and Coppenbarger, R., “NASA/FAA En Route Data Exchange (EDX) Phase 2 Field Evaluation, Project Plan,” TM 98185.04-01, Seagull Technology, Inc., February 2000.

[7] Coppenbarger, R., Weidner, T., Schleicher, D.,“En Route Data Exchange Phase 2 (EDX-2) Field Evaluation, CTAS Software Requirements, Version 2.0,” February 2000.

[8] Documentation for En Route Data Exchange (EDX) Phase 2 AMI,” Honeywell, Inc., NASA Contract No. NAS2-98001, NASA TO 25, October 1999.

[9] Slattery, R. A., Zhao, Y., “En route Descent Trajectory Synthesis for Air Traffic Control Automation,” *Proceedings of the American Control Conference*, Seattle, WA, June 1995.

[10] Coppenbarger, R. A.; Kanning, G.; and Salcido, R.; “Real-Time Data Link of Aircraft Parameters to the Center-TRACON Automation System (CTAS),” 4th USA/Europe ATM R&D Seminar, Sante Fe, NM, Dec. 3-7, 2001.

[11] Coppenbarger, R., “En-Route Climb Trajectory Prediction Enhancement Using Airline Flight-Planning Information,” AIAA-99-4147, AIAA Guidance, Navigation, and Control Conference, August 1999.

[12] D. R. Schleicher, E. Jones and R. A. Coppenbarger, NASA En Route Data Exchange Program Final Report (December 2000), FAA Prime Contract No. DTFA01-96-Y-01009, December 31, 2000.

[13] Parkinson, B., and Spilker, J., *Global Positioning System: Theory and Applications: Volume I*, Progress in Astronautics and Aeronautics-Volume 163, AIAA, Washington, DC, 1996.

[14] McVeigh, M., and Drew, D., “Accuracy of Position Data Using Mosaic Techniques,” *Journal of ATC*, January-March 2001, pp. 7-18.

[15] BAE Systems, Specification Sheet for ALLSTAR GPS Receiver, ALLSTAR DGPS-1, August, 1999.

[16] Lindsey, K., "Currency of Flight Intent Information and Impact on Trajectory Accuracy," FAA/Eurocontrol Technical Interchange Meeting on Shared Flight Intent Information and Aircraft Intent Data, October 25, 2000.

[17] Quality Engineering and Survey Technology Ltd., "Accuracy Measures," "http://www.mercat.com/QUEST/Accuracy.htm 1998.

[18] Krozel, J., Peters, M., and Hunter, G., "Conflict Detection and Resolution for Future Air Transportation Management," TR97138-01, NASA Contract NAS2-14285, Seagull Technology, Inc., Los Gatos, California, April 1997.

[19] Brudnicki, D. J., and McFarland, A. L., "User Request Evaluation Tool (URET) Conflict Probe Performance and Benefits Assessment," MITRE Center for Advanced Aviation System Development, CAASD Rept. MP98W0000112, McLean, VA, June 1997.

[20] Cale, M.L., Paglione, M., Ryan, H., Timoteo, D., and Oaks, R., "User Request Evaluation Tool (URET) Conflict Prediction Accuracy Report," Dept. of Transportation/Federal Aviation Administration, Rept. DOT/FAA/CT-TN98/8, April 1998.

[21] Weidner, T., Davidson, T.G., and Dorsky, S., "En Route Descent Advisor (EDA) and En Route Data Exchange (EDX) ATM Interruption Benefits," TR00188.26-01f, NASA Contract NAS2-98005, Seagull Technology, Inc., Los Gatos, California, December 2000.

[22] Bilimoria, K. D., "Methodology for the Performance Evaluation of a Conflict Probe," AIAA Journal of Guidance, Control, and Dynamics," Vol. 24, No. 3, May-June 2001, pp. 444-451.

[23] Weidner, T., Couluris, G., Sorensen, J., "Initial Data Link Enhancement to CTAS Build 2 Potential Benefits Analysis," TR98151-01, Seagull Technology, Los Gatos, California, June 1998.

[24] Weidner, T. J., and Mueller, T., "Comprehensive Benefits Assessment Of En Route Data Exchange (EDX)," TR00188.27-01, NASA Contract NAS2-98005, Seagull Technology, Inc., Los Gatos, California, July 2000.

[25] RTCA SC-194, "Concepts for Services Integrating Flight Operations and Air Traffic Management Using Addressed Data Link," RTCA DO-269, RTCA, Inc., Washington, DC, June 12, 2001.